

MIT Open Access Articles

Search for dark matter produced in association with a single top quark or a top quark pair in proton-proton collisions at $\sqrt{s} = 13$ TeV

The MIT Faculty has made this article openly available. **Please share** how this access benefits you. Your story matters.

Citation: Search for dark matter produced in association with a single top quark or a top quark pair in proton-proton collisions at $\sqrt{s} = 13$ TeV." Journal of High Energy Physics 2019, 3 (March 2019):141 © 2019 The Author(s)

As Published: [https://doi.org/10.1007/JHEP03\(2019\)141](https://doi.org/10.1007/JHEP03(2019)141)

Publisher: Springer Berlin Heidelberg

Persistent URL: <https://hdl.handle.net/1721.1/121282>

Version: Final published version: final published article, as it appeared in a journal, conference proceedings, or other formally published context

Terms of Use: Creative Commons Attribution



Search for dark matter produced in association with a single top quark or a top quark pair in proton-proton collisions at $\sqrt{s} = 13$ TeV



The CMS collaboration

E-mail: cms-publication-committee-chair@cern.ch

ABSTRACT: A search for dark matter produced in association with top quarks in proton-proton collisions at a center-of-mass energy of 13 TeV is presented. The data set used corresponds to an integrated luminosity of 35.9 fb^{-1} recorded with the CMS detector at the LHC. Whereas previous searches for neutral scalar or pseudoscalar mediators considered dark matter production in association with a top quark pair only, this analysis also includes production modes with a single top quark. The results are derived from the combination of multiple selection categories that are defined to target either the single top quark or the top quark pair signature. No significant deviations with respect to the standard model predictions are observed. The results are interpreted in the context of a simplified model in which a scalar or pseudoscalar mediator particle couples to a top quark and subsequently decays into dark matter particles. Scalar and pseudoscalar mediator particles with masses below 290 and 300 GeV, respectively, are excluded at 95% confidence level, assuming a dark matter particle mass of 1 GeV and mediator couplings to fermions and dark matter particles equal to unity.

KEYWORDS: Dark matter, Hadron-Hadron scattering (experiments), Top physics

ARXIV EPRINT: [1901.01553](https://arxiv.org/abs/1901.01553)

Contents

1	Introduction	1
2	The CMS detector and event reconstruction	3
3	Data sample and simulation	5
4	Event selection	6
4.1	Single-lepton signal regions	7
4.2	All-hadronic signal regions	9
4.3	Control regions	9
4.3.1	Single-lepton control regions	10
4.3.2	All-hadronic control regions	10
5	Systematic uncertainties	11
6	Signal extraction	13
7	Results	14
8	Summary	20
	The CMS collaboration	26

1 Introduction

Astrophysical observations provide evidence of the existence of nonluminous matter that can be inferred from gravitational effects on galaxies and other large scale objects in the Universe. While the nature of this dark matter (DM) is still unknown, a compelling candidate is the so-called weakly interacting massive particle [1]. This new particle is predicted to have weak interactions with standard model (SM) particles, allowing for direct- and indirect-detection experiments, as well as for searches at collider experiments.

Among all the possible interactions between the SM and DM sectors, it is of particular interest to investigate interactions mediated by a new neutral scalar or pseudoscalar particle that decays into DM particles, as these can be easily accommodated in models containing extended Higgs boson sectors [2–5]. Assuming that this DM scenario respects the principle of minimal flavor violation [6, 7], the interactions of this new spin-0 mediator particle follow the same Yukawa coupling structure as in the SM. Therefore, the mediator would couple preferentially to heavy third-generation quarks. Assuming the DM particles to be

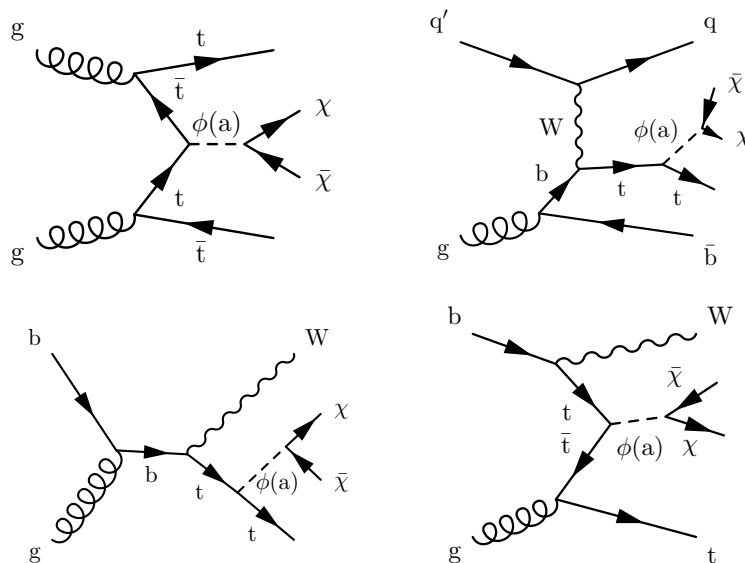


Figure 1. Principal production diagrams for the associated production at the LHC of dark matter with a top quark pair (upper left) or a single top quark with associated t channel W boson production (upper right) or with associated tW production (lower left and right).

Dirac fermions, the interaction Lagrangian terms for the production of a scalar (ϕ) or pseudoscalar (a) mediator particle can be expressed as:

$$\mathcal{L}_\phi \supset g_\chi \phi \bar{\chi} \chi + \frac{g_{q\phi}}{\sqrt{2}} \sum_f (y_f \bar{f} f), \quad (1.1)$$

$$\mathcal{L}_a \supset i g_\chi a \bar{\chi} \gamma^5 \chi + \frac{i g_{qa}}{\sqrt{2}} \sum_f (y_f \bar{f} \gamma^5 f), \quad (1.2)$$

where the sum runs over the SM fermions f , $y_f = \sqrt{2} m_f / v$ represents the Yukawa couplings, $v = 246 \text{ GeV}$ is the Higgs field vacuum expectation value, g_χ is the DM-mediator coupling, and g_q is the fermion-mediator coupling. The mediator particle subsequently decays into DM particles, which escape detection and leave an imbalance of momentum in the transverse plane, referred to as p_T^{miss} . Several theoretical studies of these types of models have been performed, in which the third-generation quark is either a top or bottom quark, leading to the production of DM in association with a pair of top ($t\bar{t}$ +DM) or bottom ($b\bar{b}$ +DM) quarks, respectively [8–11]. The main production diagram for $t\bar{t}$ +DM processes is shown in figure 1 (upper left).

Previous searches in these final states have been carried out by the ATLAS and CMS Collaborations at center-of-mass energies of 8 TeV [12, 13] and 13 TeV [14–16]. While the former results are based on an effective field theory (EFT) approach, the latter ones are interpreted in the context of simplified DM scenarios, where the mediator particle is explicitly modeled in the interaction. These interpretations have so far neglected the contribution from DM production in association with a single top quark (t/\bar{t} +DM) in which the interaction is mediated by a neutral spin-0 particle, as pointed out in ref. [17]. As in the SM, the single top quark is produced through processes mediated by a virtual t

channel (figure 1, upper right) or through associated production with a W boson (figure 1, lower left and right) [17]. While the s channel production of a W boson is also possible, this process is found to have a negligible contribution for this search. The neutral DM mediator particle is then produced either by radiation from the top quark or via top quark fusion, as described in ref. [18] for the associated production of DM with a top quark pair.

In this search, t/\bar{t} +DM processes mediated by a neutral spin-0 particle are investigated for the first time. This additional production mechanism is predicted by the same interactions described in eqs. (1.1) and (1.2) that also predict $t\bar{t}$ +DM events. For this reason, in the presented search t/\bar{t} +DM and $t\bar{t}$ +DM processes are both considered. Searches for similar final states referred to as “monotop”, which involve the production of a top quark and DM particles but without additional jets or W bosons, have been conducted by the CDF experiment [19] at the Fermilab Tevatron, by the ATLAS and CMS Collaborations [20, 21] at the CERN LHC at center-of-mass energies of 8 TeV, and at 13 TeV by the CMS Collaboration [22]. The underlying simplified models explored in these results, unlike the one presented in eqs. (1.1) and (1.2), assume either the resonant production of a $+2/3$ charged and colored spin-0 boson that decays into a right-handed top quark and one DM particle, or a spin-1 mediator with flavor changing neutral current interactions. Considering these models, in addition to the DM particle, only one top quark is assumed to be produced in the final state, unlike the t/\bar{t} +DM processes considered in this search where the top quark is produced through SM-like diagrams alongside a light quark or a W boson (figure 1).

In this paper we present a search for an excess of events above the SM background in the p_T^{miss} spectrum, as expected for the DM scenarios discussed earlier, for events that contain exactly one lepton (electron or muon) or zero leptons, henceforth assigned to the “single-lepton” (SL) region or to the “all-hadronic” (AH) region, respectively. The sensitivity of this analysis is improved beyond that of previous analyses by introducing a categorization of these signatures and new discriminating variables, as discussed in more detail in section 4.

2 The CMS detector and event reconstruction

The central feature of the CMS apparatus is a superconducting solenoid of 6 m internal diameter, providing a magnetic field of 3.8 T. Within the solenoid volume are a silicon pixel and strip tracker, a lead tungstate crystal electromagnetic calorimeter (ECAL), and a brass and scintillator hadron calorimeter (HCAL), each composed of a barrel and two endcap sections. Forward calorimeters extend the pseudorapidity (η) coverage provided by the barrel and endcap detectors. Muons are detected in gas-ionization chambers embedded in the steel flux-return yoke outside the solenoid. A more detailed description of the CMS detector, together with a definition of the coordinate system used and the relevant kinematic variables, can be found in ref. [23].

Events of interest are selected using a two-tiered trigger system [24]. The first level, composed of custom hardware processors, uses information from the calorimeters and muon detectors to select events at a rate of around 100 kHz within a time interval of less than $4\ \mu\text{s}$. The second level, known as the high-level trigger, consists of a farm of processors

running a version of the full event reconstruction software optimized for fast processing, and reduces the event rate to around 1 kHz before data storage.

The particle-flow (PF) algorithm [25] aims to reconstruct and identify each individual particle in an event, with an optimized combination of information from the various elements of the CMS detector. The energy of photons is obtained directly from the ECAL measurement and corrected for zero-suppression effects. The energy of electrons is obtained from a combination of the electron momentum at the primary interaction vertex as determined by the tracker, the energy of the corresponding ECAL cluster, and the energy sum of all bremsstrahlung photons spatially compatible with originating from the electron track. The muon track is obtained from the combination of central tracker and muon system information, and its curvature provides an estimate of the momentum. The energy of charged hadrons is determined from a combination of their momentum measured in the tracker and the matching ECAL and HCAL energy deposits, corrected for zero-suppression effects and for the response function of the calorimeters to hadronic showers. Finally, the energy of neutral hadrons is obtained from the corresponding corrected ECAL and HCAL energy.

The reconstructed vertex with the largest value of summed physics-object p_T^2 , where p_T is the transverse momentum, is taken to be the primary proton-proton (pp) interaction vertex. The physics objects are the jets and the associated \vec{p}_T^{miss} , taken as the negative vector p_T sum of those jets. For each event, hadronic jets are clustered from the particles reconstructed with PF (PF candidates) using the infrared- and collinear-safe anti- k_T algorithm [26, 27] with a distance parameter of 0.4. The jet momentum is determined as the vectorial sum of all particle momenta in the jet, and is found from simulation to be within 5 to 10% of the parton’s generated momentum over the whole p_T spectrum and detector acceptance. Additional pp interactions within the same or nearby bunch crossings (pileup) can contribute additional tracks and calorimetric energy depositions to the jet momentum. To mitigate this effect, tracks identified as originating from pileup vertices are discarded and an offset correction is applied to correct for remaining contributions [28]. Jet energy corrections are derived from simulation and applied to calibrate the jet momentum. In situ measurements of the momentum balance in dijet, photon+jet, Z+jets, and multijet events are used to account for any residual differences in jet energy scale in data and simulation [29]. Additional selection criteria are applied to each jet to remove jets potentially dominated by anomalous contributions from various subdetector components or reconstruction failures [29].

The combined secondary vertex b tagging algorithm (CSVv2) is used to identify jets originating from the hadronization of bottom quarks [30], denoted in the following as “b-tagged jets”. At the operating point of the tagging algorithm chosen for this analysis, the efficiency of identifying b quark jets in simulated $t\bar{t}$ events is about 80%, integrated over p_T , and the misidentification rate for light-flavor jets is about 1%. Scale factors are applied to the simulated samples in order to reproduce the b tagging performance measured in data.

The missing transverse momentum vector \vec{p}_T^{miss} is defined as the negative vector p_T sum of all PF particles originating from the primary vertex; its magnitude is defined as p_T^{miss} . Jet energy scale and resolution corrections are also propagated to the \vec{p}_T^{miss} calculation.

3 Data sample and simulation

The data used in this search were recorded with the CMS detector in 2016 and correspond to an integrated luminosity of 35.9 fb^{-1} . Several trigger criteria were used to collect the data, either requiring large amounts of $p_{\text{T}}^{\text{miss}}$ or the presence of at least one high- p_{T} lepton (electron or muon). Simulated samples are corrected to reproduce the observed trigger efficiencies in data.

Specifically, events that do not contain leptons are selected if they have $p_{\text{T}}^{\text{miss}}$ and missing hadronic activity $H_{\text{T}}^{\text{miss}}$ [24] above 120 GeV. This trigger is nearly 100% efficient for events with $p_{\text{T}}^{\text{miss}}$ of at least 250 GeV. The second set of triggers requires the presence of at least one isolated electron (muon) with $p_{\text{T}} > 27$ (25) GeV. The corresponding trigger efficiencies are above 90% for leptons with $p_{\text{T}} > 30$ GeV. Trigger efficiencies are measured in data.

Monte Carlo (MC) simulated samples of the main SM backgrounds and of the DM signal processes are used to optimize the event selection, assess our sensitivity to the new-physics scenarios, and form the basis of our background estimation strategy. While the detailed background composition depends on the specific channel, the main sources arise from $t\bar{t}$ +jets, W+jets, and Z+jets production. Simulated events of $t\bar{t}$ +jets production and single top quark processes are generated at next-to-leading order (NLO) in quantum chromodynamics (QCD) using POWHEG v2 and POWHEG v1 [31–33], respectively. For $t\bar{t}$ +jets processes, the top quark p_{T} distribution is reweighted to reproduce the differential cross section obtained from CMS measurements [34]. Samples of Z+jets, W+jets, and QCD multijet events are generated at leading order (LO) using MADGRAPH5_aMC@NLO [35] with the MLM prescription [36] for matching jets from the matrix element (ME) calculation to the parton shower description. Dedicated electroweak [37–42] and QCD (calculated with MADGRAPH5_aMC@NLO) NLO/LO K factors, parametrized as functions of the generated boson p_{T} , are applied to Z+jets and W+jets events. Other SM backgrounds include rare processes, such as $t\bar{t}$ +W and $t\bar{t}$ +Z, which are simulated based on the NLO ME calculations implemented in MADGRAPH5_aMC@NLO and the FxFx [43] prescription to merge multileg processes. Diboson processes (WW, WZ, ZZ, WH, ZH) are generated at NLO using either MADGRAPH5_aMC@NLO or POWHEG v2. All background samples are normalized using the most accurate cross section calculations available, which generally incorporate NLO or next-to-NLO (NNLO) precision.

The signal process is simulated at LO with the MADGRAPH5_aMC@NLO v2.4.2 event generator using a simplified model investigated within the LHC Dark Matter Forum [44]. In this model, the DM particles χ are assumed to be Dirac fermions and the mediators are spin-0 particles ϕ (a) that couple preferentially to third-generation SM quarks through scalar (pseudoscalar) couplings whose strengths are parametrized by the factor g_{q} . The coupling strength between the mediator and the DM particles is in turn given by the factor g_{χ} . This simplified model has a minimal set of four free parameters: $(m_{\chi}, m_{\phi/\text{a}}, g_{\chi}, g_{\text{q}})$, and the benchmark scenarios assume $g_{\chi} = g_{\text{q}} = 1$ as per recommendations of the LHC Dark Matter Working Group [45]. In addition, in this search we focus on the $m_{\chi} = 1 \text{ GeV}$ benchmark, which is a convenient signal reference as the production cross section

is almost independent of m_χ for on-shell mediators [44]. This simplified spin-0 model does not account for mixing between the ϕ scalar mediator and the SM Higgs boson, as discussed in ref. [46]. Under these assumptions two distinct DM scenarios are possible: the associated production with a top quark pair ($t\bar{t}$ +DM) and the associated production with a single top quark (t/\bar{t} +DM). Cross sections for both signal processes are calculated at LO with MADGRAPH5_aMC@NLO v2.4.2, with one (zero) additional partons for $t\bar{t}$ +DM (t/\bar{t} +DM) events.

For all simulated samples, the initial-state partons are modeled with the NNPDF 3.0 [47] parton distribution function (PDF) sets at LO or NLO in QCD to match the ME calculation. Generated events are interfaced with PYTHIA 8.205 [48] for parton showering and hadronization using the CUETP8M1 tune [49], except for simulated $t\bar{t}$ +jets events where the CUETP8M2 tune customized by CMS with an updated strong coupling α_S for initial-state radiation is employed [50]. All signal and background samples are processed using GEANT4 [51] to provide a full simulation of the CMS detector, including a simulation of the previously mentioned triggers. Correction factors are derived and applied to the simulated samples to match the trigger efficiencies measured in data. Additional corrections are applied to cover remaining residual differences between data and simulation that arise from the lepton identification and reconstruction efficiencies, as well as from b-tagged jet identification efficiencies.

4 Event selection

This search, similarly to a previous search for $t\bar{t}$ +DM events [16], defines several orthogonal signal regions (SRs) that are statistically combined in a simultaneous global fit of the p_T^{miss} spectrum. At the same time, various improvements are incorporated into this search to enhance the sensitivity to the t/\bar{t} +DM final state over that of previous analyses [16].

At the analysis level, jet candidates are required to have $p_T > 30$ GeV and are categorized as “central” if they lie within $|\eta| < 2.4$ and as “forward” if they are within $2.4 < |\eta| < 4.0$. The b-tagged jets identified by the CSVv2 algorithm are also required to have $p_T > 30$ GeV and in addition to lie within $|\eta| < 2.4$. Electrons and muons are selected with $p_T > 30$ GeV and $|\eta| < 2.1$. Events containing additional leptons with $p_T > 10$ GeV and $|\eta| < 2.1$ are vetoed. To ensure that candidate leptons are well-measured, identification requirements, based on hit information in the tracker and muon systems and on energy deposits in the calorimeters, are imposed. Leptons are further required to be isolated from hadronic activity, to reject leptons within jets that could arise, for example, from the decay of b quarks. A relative isolation quantity is defined as the scalar p_T sum of all PF candidates within a $\Delta R = \sqrt{(\Delta\eta)^2 + (\Delta\phi)^2}$ cone of radius 0.3 (0.4) centered around the electron (muon) candidate, where ϕ is the azimuthal angle in radians, divided by the lepton p_T [52, 53]. This relative isolation is required to be less than 0.059 (0.057) for electrons in the barrel (endcap) and less than 0.15 for muons.

Events are separated into orthogonal categories based on the number of b-tagged jets (n_b), with $n_b = 1$ or $n_b \geq 2$, and additional requirements on the number of forward jets are placed (0 or ≥ 1 forward jets) for the $n_b = 1$ category. The mentioned categorization

in terms of forward jets allows a further enhancement of t/\bar{t} +DM t channel events. In fact, as shown in figure 1, this production mode leads to final states with one top quark and an additional jet, which tends to be in the forward region of the detector, while the additionally produced b quark is typically low in p_T and therefore is not reconstructed. The minimum requirements on the number of jets is also lowered, with respect to the previous searches, to enhance the sensitivity specifically to the t/\bar{t} +DM model. Control regions (CRs) enriched in the major background processes are included in the fit in order to improve the estimates of the background contributions.

Events are classified into two “channels”, based on the number of leptons in the final state from the top quark decay: the single-lepton SL channel, containing events with exactly one electron or muon with $p_T > 30$ GeV, and the all-hadronic AH channel, containing events with exactly zero leptons with $p_T > 10$ GeV. A set of discriminating variables is identified, as discussed in more detail in sections 4.1 and 4.2 for the SL SRs and the AH SRs, respectively. The selection requirements on these variables are optimized simultaneously to increase the signal significance, using as a figure of merit the ratio between the expected number of signal and the square root of the expected SM background events. The considered signal events are either t/\bar{t} +DM events for a region that contains exactly one b -tagged jet ($n_b = 1$) or $t\bar{t}$ +DM events for a region that contains two or more b -tagged jets ($n_b \geq 2$). The region with exactly one b -tagged jet is further divided into exactly zero or ≥ 1 forward jets.

4.1 Single-lepton signal regions

Events in the SL channel are required to contain ≥ 1 identified b -tagged jet, at least 2 jets with $p_T > 30$ GeV, and $p_T^{\text{miss}} > 160$ GeV. After this selection, the dominant backgrounds in the SL channel are from $t\bar{t}$ and W +jets processes. Other backgrounds include single top quark, Drell-Yan, and diboson production.

To further improve the sensitivity and to reduce the dominant background from single-lepton $t\bar{t}$ and W +jets processes, we impose a requirement on the transverse mass m_T , calculated as:

$$m_T = \sqrt{2p_T^{\text{miss}}p_T^\ell[1 - \cos(\Delta\phi)]}, \tag{4.1}$$

where p_T^ℓ is the transverse momentum of the lepton and $\Delta\phi$ is the opening angle between the lepton direction and the p_T^{miss} vector in the transverse plane. The m_T variable is constrained by kinematic properties to be less than the W boson mass for leptonic on-shell W decays in $t\bar{t}$ and W +jets events, while for signals, off-shell W decays, or for dileptonic decays of $t\bar{t}$, the m_T variable is expected to exceed the W mass because of the additional p_T^{miss} in the event. A requirement of $m_T > 160$ GeV therefore reduces the background from single-lepton events significantly and enhances the analysis sensitivity to the DM models.

After the m_T selection, the remaining $t\bar{t}$ background is primarily from events where both top quarks decay leptonically ($t\bar{t}(2\ell)$) and one lepton is not identified. This background can be further reduced by making use of the m_{T2}^W variable [54], which is defined as the minimal value of the mass of a particle assumed to be pair produced and to decay to a W boson and a b quark jet. The W bosons are assumed to be produced on-shell and

	Single-lepton SRs			All-hadronic SRs		
	1 ℓ , 1 b-tag, 0 FJ	1 ℓ , 1 b-tag, 1FJ	1 ℓ , 2 b-tag	0 ℓ , 1 b-tag, 0 FJ	0 ℓ ,1 b-tag, 1 FJ	0 ℓ , 2 b-tag
Forward jets	=0	≥ 1	—	= 0	≥ 1	—
n_b	=1	=1	≥ 2	= 1	=1	≥ 2
n_{lep}	=1	=1	=1	= 0	=0	=0
$p_T(j_1)/H_T$		—			—	< 0.5
n_{jet}		≥ 2			≥ 3	
p_T^{miss}		> 160 GeV			> 250 GeV	
m_T		> 160 GeV			—	
m_{T2}^W		> 200 GeV			—	
$\min\Delta\phi(j_{1,2}, \vec{p}_T^{miss})$		> 1.2 rad.			> 1.0 rad.	
m_T^b		> 180 GeV			> 180 GeV	

Table 1. Final event selections for the SL and AH SRs. Electrons and muons are kept separate for the SL channel.

to decay leptonically, where one of the two leptons is not detected. Based on the variable definition, in $t\bar{t}(2\ell)$ events the m_{T2}^W distribution has a kinematic end point at the top quark mass, assuming perfect detector response, while this is not the case for signal events where two additional DM particles are present. The calculation of m_{T2}^W requires two b-tagged jets from the decay of the top quarks, where one of these b-tagged jets comes from the same decay chain as the reconstructed lepton. If only one b-tagged jet is identified in the event, each of the first three (or two in three-jet events) leading non-b-tagged jets is considered as the second b-tagged jet in the calculation. The m_{T2}^W is then evaluated for all possible jet-lepton combinations and the minimum m_{T2}^W value is considered to discriminate between signal and background events. If two or more b-tagged jets are identified in the events, all b-tagged jets are considered and similarly all possible jet-lepton combinations are used to calculate m_{T2}^W values. The smallest of all the m_{T2}^W values is taken as the event discriminant.

In addition, jets and the \vec{p}_T^{miss} vector tend to be more separated in the transverse plane in signal events than in $t\bar{t}$ background processes. To improve the search sensitivity, the minimum opening angle $\min\Delta\phi(j_{1,2}, \vec{p}_T^{miss})$ in the transverse plane between the direction of each of the first two leading- p_T jets with $|\eta| < 2.4$ and the \vec{p}_T^{miss} vector is required to be greater than 1.2 radians.

The $t\bar{t}$ background is further reduced by requiring that the transverse mass m_T^b of the \vec{p}_T^{miss} vector and of a b-tagged jet is greater than 180 GeV, where m_T^b is defined similarly to eq. (4.1) but considering a b-tagged jet instead of a lepton. In fact, for the remaining $t\bar{t}$ background m_T^b tends to have values below or around the top quark mass if the b-tagged jet belongs to the top quark whose lepton is not identified. For the calculation we choose the b-tagged jet with the highest CSVv2 discriminant value, if there is more than one candidate.

A summary of the selection criteria for the SL SRs is shown in the first three columns of table 1. Each region is identified by a unique name, where 0 ℓ denotes exactly zero leptons, 1(2) b-tag represents exactly 1 (at least 2) b-tagged jet, and 0 FJ or 1 FJ denotes exactly zero or at least one forward jet.

4.2 All-hadronic signal regions

Events categorized into the AH channel must contain at least 1 identified b-tagged jet and at least 3 jets with $p_T > 30$ GeV, $p_T^{\text{miss}} > 250$ GeV, and $\min\Delta\phi(j_{1,2}, \vec{p}_T^{\text{miss}})$ greater than 0.4 radians.

The dominant backgrounds after this selection arise from $t\bar{t}$, W+jets, and $Z \rightarrow \nu\nu$ processes. Other backgrounds include QCD multijet events, single top quark, Drell-Yan, and diboson production.

Semileptonic $t\bar{t}$ events populate this channel if the lepton in the final state is not identified. This $t\bar{t}(1\ell)$ background is reduced by applying the same m_T^b selection as introduced in the SL channel. To further reduce the $t\bar{t}(1\ell)$ background, together with that from $Z \rightarrow \nu\nu$ events, we make use of the $p_T(j_1)/H_T$ variable, which is defined as the ratio of the leading p_T jet in the event divided by the total hadronic transverse energy in the event, H_T , which is the scalar p_T sum of the jets with $p_T > 30$ GeV within $|\eta| < 2.4$. In the case of background, the distribution peaks at higher values with respect to $t\bar{t}$ +DM signal events. The t/\bar{t} +DM events, however, tend to exhibit a distribution similar to that of the background. Events in the $n_b \geq 2$ category are required to have $p_T(j_1)/H_T < 0.5$.

For QCD multijet events no intrinsic p_T^{miss} is expected. Therefore, events that pass our minimum p_T^{miss} selection contain mostly p_T^{miss} which arises from jet mismeasurements. For these events, the p_T^{miss} is often aligned with one of the leading jets. As a result, selecting events with $\min\Delta\phi(j_{1,2}, \vec{p}_T^{\text{miss}})$ values greater than 1 radian reduces the background from QCD multijet production. This contribution to the SR, estimated through simulated samples, is negligible. The description of the QCD multijet background basic kinematic distributions is verified in a dedicated region enriched in multijet events, obtained by reversing the $\min\Delta\phi(j_{1,2}, \vec{p}_T^{\text{miss}})$ selection, and the simulation is found to model the data well.

A summary of the selection criteria for the AH SRs is shown in the last three columns of table 1. Each region is identified by a unique name, where 1ℓ denotes exactly one muon or one electron, 1(2) b-tag represents exactly 1 (at least 2) b-tagged jet, and 0 FJ or 1 FJ denotes exactly zero or at least one forward jet.

4.3 Control regions

After events are categorized according to the selection presented in table 1, the expected SM backgrounds in these different regions must be evaluated. In the SL SRs, the main backgrounds are dileptonic $t\bar{t}$ events, where one lepton is not identified, and W+jets events. For the AH regions the main backgrounds arise instead from single-lepton $t\bar{t}$ and W+jets events, where the lepton is not identified, and Z boson production, where the Z boson decays into two neutrinos and leads to a background with genuine p_T^{miss} .

In order to improve the estimation of these main backgrounds, methods based on control samples in data are used. In particular, CRs enhanced in the different background sources are used to derive correction factors as a function of the p_T^{miss} from the comparison of the p_T^{miss} distribution between the data and the simulation. These corrections are extracted and simultaneously propagated across the CRs and SRs for a given channel in the context

	Single-lepton CRs		All-hadronic CRs		
	CR $t\bar{t}(2\ell)$	CR $W(\ell\nu)$	CR $t\bar{t}(1\ell)$	CR $W(\ell\nu)$	CR $Z(\ell\ell)$
n_b	≥ 1	$= 0$	≥ 1	$= 0$	$= 0$
n_{lep}	$= 2$	$= 1$	$= 1$	$= 1$	$= 2$
n_{jet}	≥ 2	≥ 2	≥ 3	≥ 3	≥ 3
p_T^{miss}	> 160 GeV	> 160 GeV	> 250 GeV	> 250 GeV	> 250 GeV
m_T	—	> 160 GeV	< 160 GeV	< 160 GeV	—
$\min\Delta\phi(j_{1,2}, \vec{p}_T^{miss})$	—	—	> 1.0 rad.	—	—
$m_{\ell\ell}$	—	—	—	—	[60, 120] GeV

Table 2. Control regions defined for the main backgrounds of the SL SRs (first two columns, $t\bar{t}(2\ell)$ and W +jets) and the AH SRs (last 3 columns, $t\bar{t}(1\ell)$, W +jets, and $Z \rightarrow \ell\ell$). Some selections applied in the SRs are removed in the corresponding CRs to increase the available statistics and are therefore not listed. The p_T^{miss} selection for the $Z \rightarrow \ell\ell$ CR refers to the hadronic recoil.

of a global fit, as explained in more detail in section 6. The residual background processes are modeled with simulation.

The background CRs for the SL and AH channels are designed to be statistically independent from the corresponding SRs.

4.3.1 Single-lepton control regions

The first set of CRs is defined to isolate dileptonic $t\bar{t}$ events by requiring exactly two leptons (1 electron and 1 muon, 2 electrons, or 2 muons), $n_{jet} \geq 2$, $n_b \geq 1$, and $p_T^{miss} > 160$ GeV. In order to statistically enhance these CRs the m_T , m_{T2}^W , and forward jet selections are removed.

The second set of CRs is designed to isolate W +jets events by requiring exactly one lepton (electron or muon), $n_{jet} \geq 2$, $n_b = 0$, $p_T^{miss} > 160$ GeV, and $m_T > 160$ GeV. The $n_b = 0$ requirement makes this CR orthogonal to the SL SR and allows the events in the m_T tail to be modeled without extrapolation from a lower- m_T region.

Both of these selections are summarized in the first two columns of table 2.

4.3.2 All-hadronic control regions

For the AH SRs, three independent sets of CRs are defined. The first set of CRs is enhanced in single-lepton $t\bar{t}$ events selecting events with exactly one lepton (electron or muon), $n_{jet} \geq 3$, $n_b \geq 1$, $p_T^{miss} > 250$ GeV, and, in order to avoid overlap with the SL SRs, $m_T < 160$ GeV.

The second set of CRs is defined to enhance single-lepton W +jets events. Events are selected with exactly one lepton (electron or muon), $n_{jet} \geq 3$, $n_b = 0$, $p_T^{miss} > 250$ GeV, and in order to avoid overlap with the SL W +jets CR, $m_T < 160$ GeV.

The third and last set of CRs are designed to model the background due to Z +jets production, where the Z boson decays into a pair of neutrinos ($Z \rightarrow \nu\nu$). Here we use the Z boson decays to an opposite-sign, same-flavor dilepton pair ($Z \rightarrow \ell\ell$), as proxy events to emulate the kinematic properties of the Z +jets process. Events are selected requiring 2 leptons, which have the same flavor (i.e., ee or $\mu\mu$), and opposite charge, and that satisfy a requirement on their invariant mass of $60 < m_{\ell\ell} < 120$ GeV. Additionally, events must

contain at least 3 jets, but events with b-tagged jets are vetoed ($n_b = 0$). In order to reproduce the p_T spectrum of $Z \rightarrow \nu\nu$ events, the two leptons are added to the \vec{p}_T^{miss} , referred to as hadronic recoil.

A summary of the different AH CRs can be found in the last three columns of table 2.

5 Systematic uncertainties

Several sources of uncertainty are considered that affect either the simulation of the background processes or the underlying theoretical modeling. We distinguish between two types of uncertainties, ones that only affect the normalization of a process and others that additionally affect the shape of the p_T^{miss} distribution. All of these uncertainties are included in the global simultaneous fit, described in detail later. The largest impacts on the final results stem from the uncertainties in the b tagging scale factors and the limited statistical precision of the dilepton $t\bar{t}$ CR, where the latter is the main determining factor for the contribution of $t\bar{t}$ events in the SL SRs.

The following sources of uncertainty correspond to constrained normalization nuisance parameters in the fit (unless specified, the source of uncertainty applies to all search channels):

- *Lepton reconstruction, selection, and trigger.* Scale factors are applied to the simulation in order to mimic the measured lepton reconstruction and selection efficiencies in data. The measured uncertainties in these scale factors are of the order of 2.2% per electron and 1% per muon, and are p_T and η dependent [52, 53]. The effect of these uncertainties is found to be independent of the p_T^{miss} spectrum.
- *p_T^{miss} trigger.* At values of $p_T^{\text{miss}} > 250$ GeV the applied triggers are almost fully efficient; a normalization uncertainty of 2% is assigned. This uncertainty is only applied in the AH channel.
- *b tagging efficiency scale factors.* The b tagging and light-flavor mistag efficiencies scale factors and the respective uncertainties are measured in independent control samples [30], and propagated to the analysis. In the range of p_T^{miss} considered, these scale factor uncertainties do not alter the shape of the p_T^{miss} distribution.
- *Forward jets.* Inclusive CRs in terms of forward jet multiplicity are considered to constrain the major background in the 0 and ≥ 1 forward jets SRs. The impact of this extrapolation in forward jets multiplicity on the background estimation is evaluated and assigned as additional systematic uncertainty. The extrapolation effect is evaluated by splitting each CR into a 0f and 1f category, and a systematic uncertainty is assigned based on the ratio of the correction factors, where each correction factor is the ratio of the data to the simulation in its category. This uncertainty ranges from approximately 2% (W+jets AH) to about 7% ($t\bar{t}$ SL).
- *Pileup modeling.* Systematic uncertainties due to pileup modeling are taken into account by varying the total inelastic cross section used to calculate pileup distributions in simulation by $\pm 4.6\%$ [55].

- *Luminosity.* An uncertainty of 2.5% is taken on the integrated luminosity of the data sample [56].
- *QCD multijet background normalization.* An uncertainty of 100% in the normalization is considered for QCD processes to cover effects in the kinematic tails that may not be well-modeled by the simulation. This has little overall impact on the final result, since the contribution from QCD multijet events is reduced to a negligible amount in this analysis.
- *Single top quark background normalization.* An uncertainty of 20% in the normalization is considered for single top quark processes, accounting for the uncertainty in the PDF and the effects from varying the factorization and renormalization scale parameters.
- *Uncertainty related to ECAL mistiming.* Partial mistiming of signals in the forward regions of the ECAL endcaps led to a minor reduction in trigger efficiency. To cover this effect, an additional uncertainty is applied on the signal acceptances of up to 10% in the forward jet categories. A potential effect on the background extrapolation into regions with forward jets is already taken into account by a dedicated systematic uncertainty.

The following sources of uncertainty affect the shape of the p_T^{miss} distribution, as well as the normalization of the various backgrounds and the signal, and are applied to all search channels:

- *Jet energy scale.* Reconstructed jet four-momenta in the simulation are varied according to the uncertainty in the jet energy scale. Jet energy scale uncertainties are coherently propagated to all observables, including p_T^{miss} [57].
- *PDF uncertainties.* Uncertainties due to the choice of PDF are estimated by reweighting the samples with the NNPDF3.0 [47] replicas [58] and are applied to all backgrounds except for the single top quark, as these uncertainties are covered by the associated background normalization uncertainty.
- *W/Z+heavy-flavor fraction.* The uncertainty in the fraction of W/Z+heavy-flavor (HF) jets in W+jets and Z+jets event is taken into account. The relative contribution of W+HF and Z+HF are allowed to vary within 20% [59–62].
- *Electroweak and QCD K factors.* Uncertainties in the NLO/LO K factors calculated for W+jets and Z+jets processes are considered. These uncertainties account for missing higher-order corrections. For QCD, this comes from variations due to factorization and renormalization scales. For electroweak processes, an estimate of the size of the missing higher-order corrections is obtained by taking the difference between applying and not applying the NLO/LO electroweak K factors.
- *Top quark p_T reweighting.* Differential measurements of the top quark p_T spectrum in top quark pair production events [34] show that the measured p_T spectrum is

softer than in simulation. In order to improve the description of top quark pair events, simulated samples are reweighted to match the measurements. An associated systematic uncertainty is estimated by taking the difference between applying and not applying the reweighting.

- *Factorization and renormalization scales.* The uncertainties in the choice of the factorization and renormalization scale parameters are taken into account for the $t\bar{t}$, $t\bar{t}+V$, and diboson processes by applying a set of weights that represent a change of these scales by a factor of 2 or 0.5.
- *Simulation sample size.* Uncertainties due to the limited size of the simulated signal and background samples are included by allowing each bin of the distributions used in the signal extraction to fluctuate independently according to the statistical uncertainties in simulation, following ref. [63].

6 Signal extraction

As previously discussed, the potential DM signal is expected to have the signature of $t\bar{t}$ or single top quark events with additional p_T^{miss} , therefore leading to an excess of events above the SM prediction in the p_T^{miss} spectrum. The DM signal is extracted from a simultaneous fit to the binned p_T^{miss} distribution in the various SRs and CRs, including all previously mentioned uncertainties. This global fit is performed as a binned maximum likelihood fit employing the ROOSTATS statistical package [64]. The main SM backgrounds were discussed previously in section 4, and are dileptonic $t\bar{t}$ +jets and W +jets events for the SL SRs, and $Z \rightarrow \nu\nu$, single-lepton $t\bar{t}$ +jets, and W +jets events for the AH SRs.

The effect of the systematic uncertainties in the shape and normalization of the p_T^{miss} spectrum, as discussed in the previous section, is taken into account by introducing nuisance parameters, which are constrained by the magnitude of the corresponding source of uncertainty. Uncertainties that affect normalization only are modeled using nuisances with log-normal probability densities. These parameters are treated as correlated between p_T^{miss} bins and between the different CRs and SRs within each channel. The sources common between SL and AH SRs and CRs are correlated across channels.

To improve the estimation of the main backgrounds, an unconstrained multiplicative parameter is assigned separately to each background for each bin of the p_T^{miss} spectrum. These multiplicative parameters scale the normalization of the associated background process simultaneously in the SRs and CRs for a given channel. For example, in a given p_T^{miss} bin of the SL selection, there is one multiplicative parameter for $t\bar{t}$ that links the $t\bar{t}$ background in the $t\bar{t}$ enhanced 2ℓ CR, the W +jets enhanced 1ℓ CR, and the SR. Therefore, the effect of contributions of the same background process in the different CRs is also taken into account. Additionally, potential contributions from the DM signals are included for all CRs and SRs, and scaled by a signal strength modifier $\mu = \sigma/\sigma_{\text{th}}$, i.e., the ratio between the measured and theoretical cross sections. Regions containing leptons (electrons and muons) are separated by lepton flavor.

The simultaneous fit to the binned p_T^{miss} distribution is performed combining the SL and AH regions. The values for the background multiplicative factors extracted from the fit are on average close to one, with a root-mean-square deviation that ranges from 5% to 21%, depending on the background processes and on the category considered (SL or AH). The post-fit distributions assuming the absence from the DM signal (i.e., the background only fit) are shown in figures 2 and 3 (4 and 5) for the SL and AH CRs (SRs), respectively. No significant excess at high p_T^{miss} in the SRs is observed. The SRs, both for the SL and AH channels, are divided into: 1 b-tagged jet and 0 forward jets, 1 b-tagged jet and ≥ 1 forward jets, and ≥ 2 b-tagged jets. The plots also contain the pre-fit distributions, represented by the dashed magenta line. The statistical and systematic uncertainties in the prediction are represented by hatched uncertainty bands, while the lower panels show the ratio of data and the post-fit prediction, and the bottom panels show the difference between the observed data events and the post-fit total background, divided by the full statistical and systematic uncertainty.

7 Results

Overall, data are found to be in agreement with the expected SM background in the SRs. Upper limits at 95% confidence level (CL) are computed on the ratio between the measured and theoretical cross sections μ , which is calculated with respect to the expected number of events for a scalar or pseudoscalar mediator and either the t/\bar{t} +DM or $t\bar{t}$ +DM production modes separately, or summed together, where the results are referred to here as t , $t\bar{t}$ +DM. The theoretical cross sections for both signal models are obtained at LO. The limits are calculated using a modified frequentist approach with a test statistic based on the profile likelihood in the asymptotic approximation and the CL_s criterion [65–67]. We test different mediator mass scenarios with $m_\chi = 1$ GeV and $g_q = g_\chi = 1$ and the results are shown in figure 6 for scalar (left) and pseudoscalar (right) models. The expected limit for the t/\bar{t} +DM signal alone is depicted by the blue dash-dotted line, while the expected $t\bar{t}$ +DM limit alone is given by the red dash-dotted line. The observed limit on the sum of both signals is represented by the black solid line, while its expected value is shown by the black dashed line with the 68 and 95% CL uncertainty bands in green and yellow, respectively.

For masses of the mediator particle below 200 GeV for the scalar model and below 300 GeV for the pseudoscalar model, the leading contribution to the sensitivity of the analysis stems from $t\bar{t}$ +DM. This behavior is mostly driven by the larger cross section for the $t\bar{t}$ +DM process when compared to the sum of the production processes for t/\bar{t} +DM. However, the t/\bar{t} +DM cross section drops less rapidly as a function of mediator particle mass in comparison to the $t\bar{t}$ +DM mode. Additionally, the p_T^{miss} spectrum for a given mediator mass leans towards higher values for the t/\bar{t} +DM signal model when compared to the $t\bar{t}$ +DM model. These two features, together with the analysis specifically designed for both DM production modes and the statistical combination of the different SRs, lead up to a factor of two improvement at high mediator masses on the limits when compared to previous results [16]. In particular, the ≥ 1 forward jet category, which is specifically designed to enhance t/\bar{t} +DM t channel events, improves the final results up to 14%.

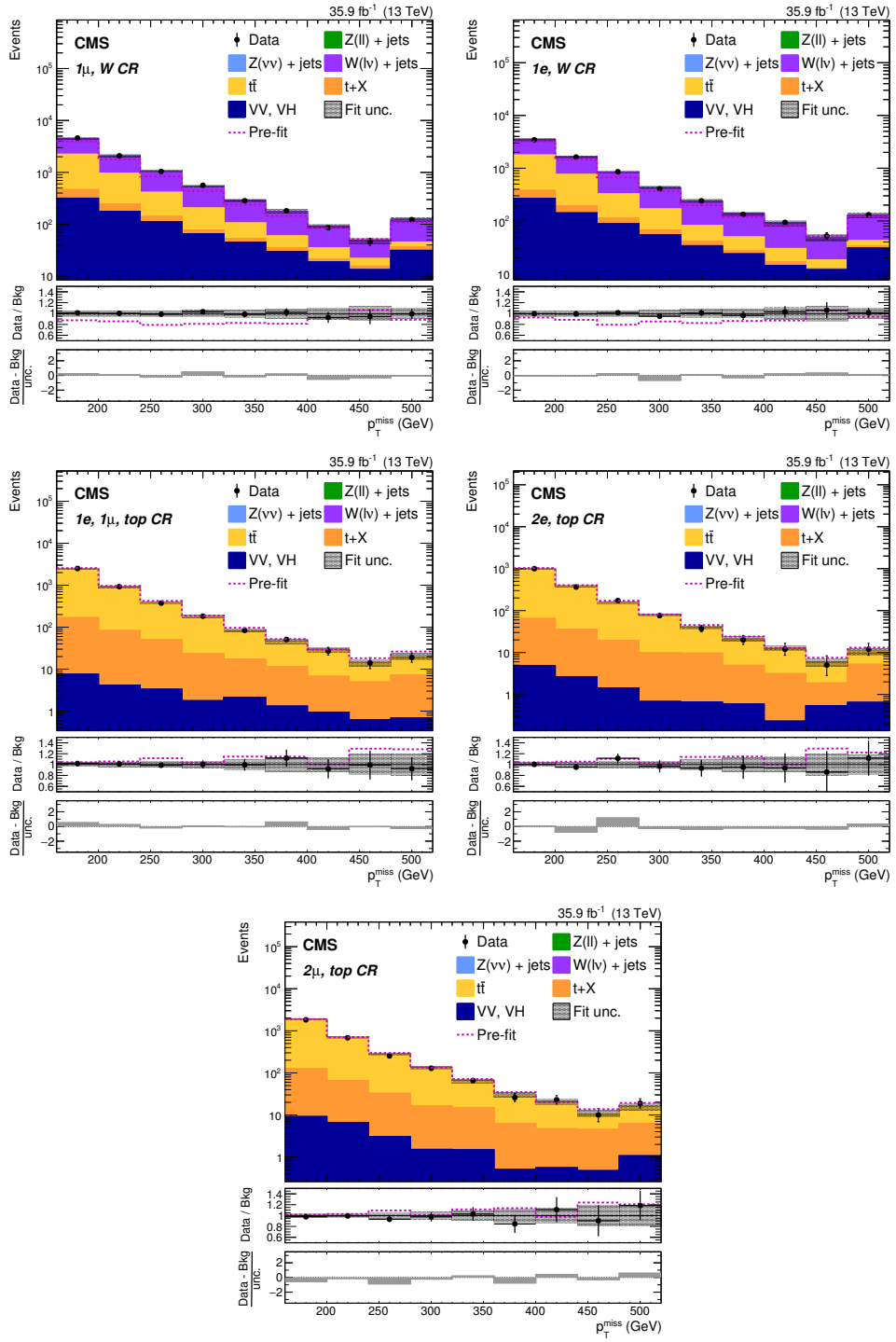


Figure 2. Background-only post-fit p_T^{miss} distributions for the CRs of the SL selection. The total theory signal ($t\bar{t}+\text{DM}$ and $t\bar{t}+\text{DM}$ summed together) is negligible and therefore is not shown. The last bin contains overflow events. The dashed magenta lines show the total pre-fit background expectation in the upper panels, and the ratio of pre-fit total background to post-fit total background in the middle panels. The lower panels show the difference between observed and post-fit total background divided by the full statistical and systematic uncertainties.

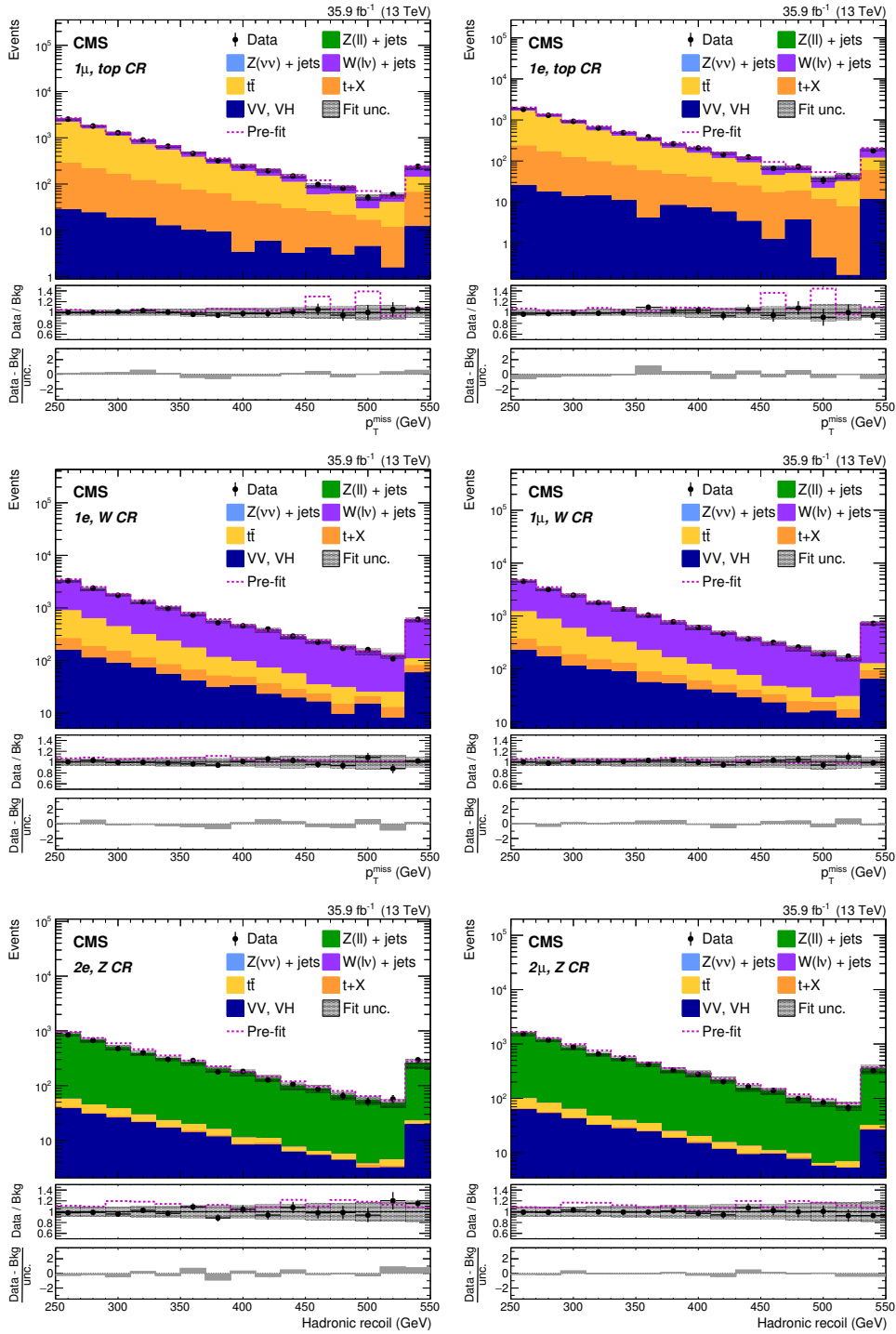


Figure 3. Background-only post-fit p_T^{miss} distributions for the CRs of the AH selection. The total theory signal ($t/\bar{t}+\text{DM}$ and $t\bar{t}+\text{DM}$ summed together) is negligible and therefore is not shown. The last bin contains overflow events. The dashed magenta lines show the total pre-fit background expectation in the upper panels, and the ratio of pre-fit total background to post-fit total background in the middle panels. The lower panels show the difference between observed and post-fit total background divided by the full statistical and systematic uncertainties.

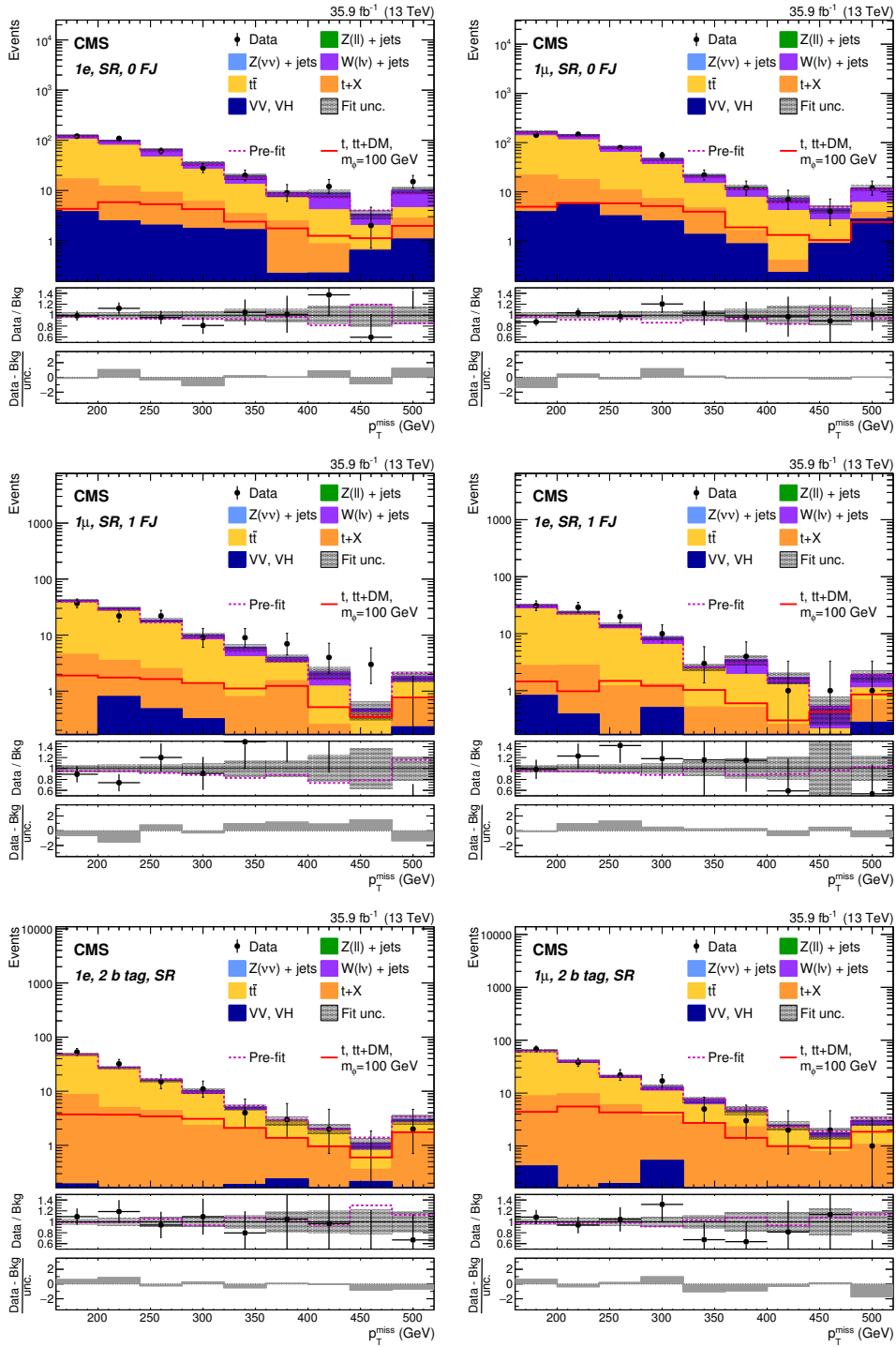


Figure 4. Background-only post-fit p_T^{miss} distributions for the SRs of the SL selection. The total theory signal ($t/\bar{t}+\text{DM}$ and $t\bar{t}+\text{DM}$ summed together) is presented by the red solid lines for a scalar mediator mass of 100 GeV. The last bin contains overflow events. The dashed magenta lines show the total pre-fit background expectation in the upper panels, and the ratio of pre-fit total background to post-fit total background in the middle panels. The lower panels show the difference between observed and post-fit total background divided by the full statistical and systematic uncertainties.

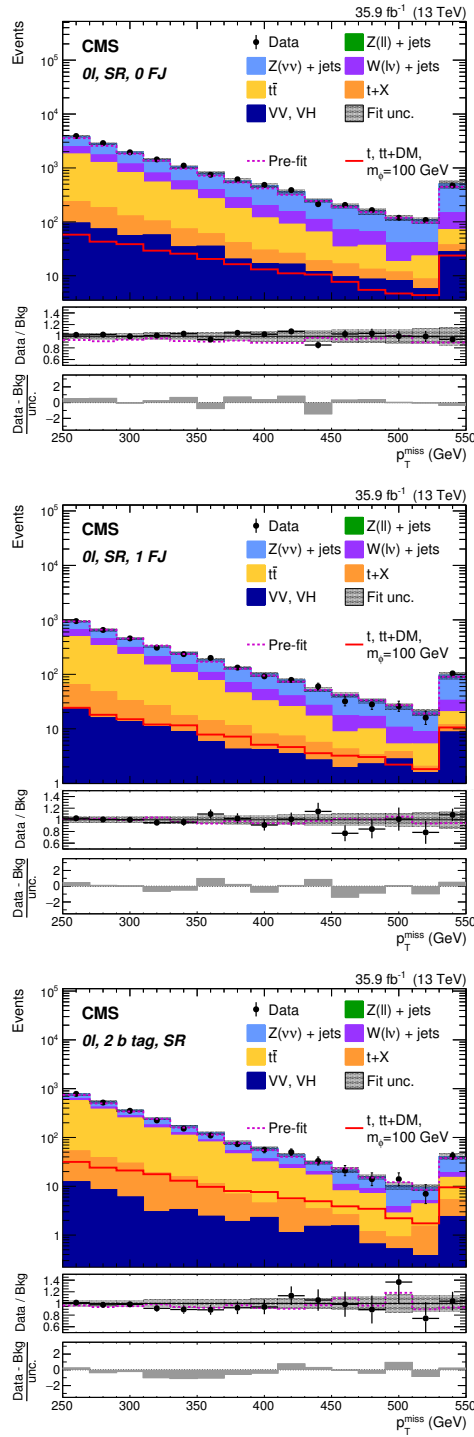


Figure 5. Background-only post-fit p_T^{miss} distributions for the SRs of the AH selection. The total theory signal ($t/\bar{t}+\text{DM}$ and $t\bar{t}+\text{DM}$ summed together) is presented by the red solid lines for a scalar mediator mass of 100 GeV. The last bin contains overflow events. The dashed magenta lines show the total pre-fit background expectation in the upper panels, and the ratio of pre-fit total background to post-fit total background in the middle panels. The lower panels show the difference between observed and post-fit total background divided by the full statistical and systematic uncertainties.

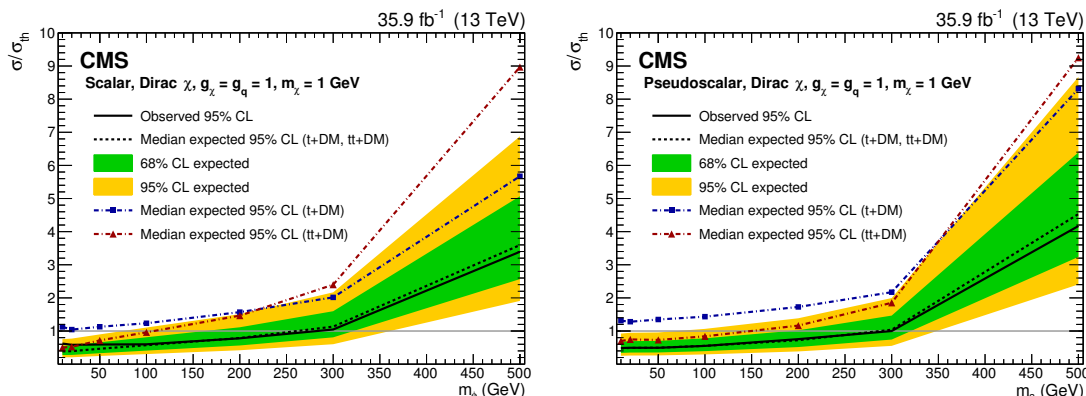


Figure 6. The expected and observed 95% CL limits on the DM production cross sections, relative to the theory predictions, shown for the scalar (left) and pseudoscalar (right) models. The expected limit for the t/\bar{t} +DM signal alone is depicted by the blue dash-dotted line, while the $t\bar{t}$ +DM limit alone is given by the red dash-dotted line. The observed limit on the sum of both signals is shown by the black solid line, while the expected value is shown by the black dashed line with the 68 and 95% CL uncertainty bands in green and yellow, respectively. The solid horizontal line corresponds to $\sigma/\sigma_{\text{th}} = 1$.

	$m_{\phi/a}(\text{GeV})$	t/\bar{t} +DM		$t\bar{t}$ +DM		$t, t\bar{t}$ +DM sum			
		Obs.	Exp.	Obs.	Exp.	Obs.	Exp.	68% CI	95% CI
Scalar	10	1.59	1.12	0.91	0.50	0.62	0.39	[0.27, 0.55]	[0.21, 0.76]
	20	1.38	1.04	0.84	0.52	0.58	0.39	[0.28, 0.56]	[0.21, 0.77]
	50	1.15	1.13	1.11	0.72	0.59	0.46	[0.33, 0.66]	[0.25, 0.90]
	100	1.43	1.23	0.94	0.96	0.60	0.57	[0.41, 0.81]	[0.30, 1.11]
	200	1.66	1.57	1.37	1.46	0.78	0.79	[0.56, 1.11]	[0.42, 1.51]
	300	1.97	2.02	2.09	2.40	1.05	1.13	[0.81, 1.60]	[0.60, 2.17]
Pseudoscalar	500	5.84	5.67	7.48	8.97	3.39	3.59	[2.57, 5.07]	[1.91, 6.88]
	10	1.43	1.31	0.70	0.70	0.49	0.47	[0.34, 0.67]	[0.25, 0.92]
	20	1.43	1.28	0.71	0.75	0.49	0.49	[0.35, 0.70]	[0.26, 0.95]
	50	1.48	1.35	0.70	0.73	0.49	0.50	[0.35, 0.70]	[0.26, 0.96]
	100	1.53	1.43	0.81	0.84	0.55	0.55	[0.39, 0.78]	[0.29, 1.06]
	200	1.89	1.73	1.18	1.16	0.76	0.72	[0.52, 1.02]	[0.38, 1.38]
	300	2.17	2.17	1.74	1.85	1.00	1.04	[0.74, 1.47]	[0.55, 2.00]
	500	8.22	8.31	8.00	9.25	4.17	4.53	[3.24, 6.39]	[2.41, 8.67]

Table 3. Upper limits at 95% CL on the cross section ratio with respect to the expected DM signal for different scalar (ϕ) or pseudoscalar (a) mediator masses, $m_\chi = 1$ GeV, and $g_\chi = g_q = 1$ for the combination of SL and AH signal regions. The median expected value and its 68 and 95% confidence intervals (CIs) are given.

Table 3 represents the final combined limits (SL + AH) for the t/\bar{t} +DM and $t\bar{t}$ +DM processes separately, and for the sum of the two processes.

Overall, we exclude mediator masses below 290 and 300 GeV for the scalar and pseudoscalar hypotheses, respectively.

8 Summary

The first search at the LHC for dark matter (DM) produced in association with a single top quark or a top quark pair in interactions mediated by a neutral scalar or pseudoscalar particle in proton-proton collisions at a center-of-mass energy of 13 TeV has been presented. The data correspond to an integrated luminosity of 35.9 fb^{-1} recorded by the CMS experiment in 2016. No significant deviations with respect to standard model predictions are observed and the results are interpreted in the context of a simplified model in which a scalar or pseudoscalar mediator particle couples to the top quark and subsequently decays into two DM particles.

Scalar and pseudoscalar mediator masses below 290 and 300 GeV are excluded at 95% confidence level assuming a DM particle mass of 1 GeV and mediator couplings to fermions and DM particles equal to unity. This analysis provides the most stringent limits derived at the LHC for these new spin-0 mediator particles.

Acknowledgments

We congratulate our colleagues in the CERN accelerator departments for the excellent performance of the LHC and thank the technical and administrative staffs at CERN and at other CMS institutes for their contributions to the success of the CMS effort. In addition, we gratefully acknowledge the computing centres and personnel of the Worldwide LHC Computing Grid for delivering so effectively the computing infrastructure essential to our analyses. Finally, we acknowledge the enduring support for the construction and operation of the LHC and the CMS detector provided by the following funding agencies: BMBWF and FWF (Austria); FNRS and FWO (Belgium); CNPq, CAPES, FAPERJ, FAPERGS, and FAPESP (Brazil); MES (Bulgaria); CERN; CAS, MoST, and NSFC (China); COLCIENCIAS (Colombia); MSES and CSF (Croatia); RPF (Cyprus); SENESCYT (Ecuador); MoER, ERC IUT, and ERDF (Estonia); Academy of Finland, MEC, and HIP (Finland); CEA and CNRS/IN2P3 (France); BMBF, DFG, and HGF (Germany); GSRT (Greece); NKFIA (Hungary); DAE and DST (India); IPM (Iran); SFI (Ireland); INFN (Italy); MSIP and NRF (Republic of Korea); MES (Latvia); LAS (Lithuania); MOE and UM (Malaysia); BUAP, CINVESTAV, CONACYT, LNS, SEP, and UASLP-FAI (Mexico); MOS (Montenegro); MBIE (New Zealand); PAEC (Pakistan); MSHE and NSC (Poland); FCT (Portugal); JINR (Dubna); MON, RosAtom, RAS, RFBR, and NRC KI (Russia); MESTD (Serbia); SEIDI, CPAN, PCTI, and FEDER (Spain); MOSTR (Sri Lanka); Swiss Funding Agencies (Switzerland); MST (Taipei); ThEPCenter, IPST, STAR, and NSTDA (Thailand); TUBITAK and TAEK (Turkey); NASU and SFFR (Ukraine); STFC (United Kingdom); DOE and NSF (U.S.A.).

Individuals have received support from the Marie-Curie programme and the European Research Council and Horizon 2020 Grant, contract No. 675440 (European Union); the Leventis Foundation; the A.P. Sloan Foundation; the Alexander von Humboldt Foundation; the Belgian Federal Science Policy Office; the Fonds pour la Formation à la Recherche dans l'Industrie et dans l'Agriculture (FRIA-Belgium); the Agentschap voor Innovatie door

Wetenschap en Technologie (IWT-Belgium); the F.R.S.-FNRS and FWO (Belgium) under the “Excellence of Science — EOS” — be.h project n. 30820817; the Ministry of Education, Youth and Sports (MEYS) of the Czech Republic; the Lendület (“Momentum”) Programme and the János Bolyai Research Scholarship of the Hungarian Academy of Sciences, the New National Excellence Program ÚNKP, the NKFI research grants 123842, 123959, 124845, 124850, and 125105 (Hungary); the Council of Science and Industrial Research, India; the HOMING PLUS programme of the Foundation for Polish Science, cofinanced from European Union, Regional Development Fund, the Mobility Plus programme of the Ministry of Science and Higher Education, the National Science Center (Poland), contracts Harmonia 2014/14/M/ST2/00428, Opus 2014/13/B/ST2/02543, 2014/15/B/ST2/03998, and 2015/19/B/ST2/02861, Sonata-bis 2012/07/E/ST2/01406; the National Priorities Research Program by Qatar National Research Fund; the Programa Estatal de Fomento de la Investigación Científica y Técnica de Excelencia María de Maeztu, grant MDM-2015-0509 and the Programa Severo Ochoa del Principado de Asturias; the Thalís and Aristeia programmes cofinanced by EU-ESF and the Greek NSRF; the Rachadapisek Sompot Fund for Postdoctoral Fellowship, Chulalongkorn University and the Chulalongkorn Academic into Its 2nd Century Project Advancement Project (Thailand); the Welch Foundation, contract C-1845; and the Weston Havens Foundation (U.S.A.).

Open Access. This article is distributed under the terms of the Creative Commons Attribution License ([CC-BY 4.0](https://creativecommons.org/licenses/by/4.0/)), which permits any use, distribution and reproduction in any medium, provided the original author(s) and source are credited.

References

- [1] G. Bertone, D. Hooper and J. Silk, *Particle dark matter: evidence, candidates and constraints*, *Phys. Rept.* **405** (2005) 279 [[hep-ph/0404175](#)] [[INSPIRE](#)].
- [2] Y.G. Kim, K.Y. Lee, C.B. Park and S. Shin, *Secluded singlet fermionic dark matter driven by the Fermi gamma-ray excess*, *Phys. Rev. D* **93** (2016) 075023 [[arXiv:1601.05089](#)] [[INSPIRE](#)].
- [3] A. Berlin, S. Gori, T. Lin and L.-T. Wang, *Pseudoscalar portal dark matter*, *Phys. Rev. D* **92** (2015) 015005 [[arXiv:1502.06000](#)] [[INSPIRE](#)].
- [4] Y.G. Kim, K.Y. Lee and S. Shin, *Singlet fermionic dark matter*, *JHEP* **05** (2008) 100 [[arXiv:0803.2932](#)] [[INSPIRE](#)].
- [5] L. Lopez-Honorez, T. Schwetz and J. Zupan, *Higgs portal, fermionic dark matter and a Standard Model like Higgs at 125 GeV*, *Phys. Lett. B* **716** (2012) 179 [[arXiv:1203.2064](#)] [[INSPIRE](#)].
- [6] G. D’Ambrosio, G.F. Giudice, G. Isidori and A. Strumia, *Minimal flavor violation: an effective field theory approach*, *Nucl. Phys. B* **645** (2002) 155 [[hep-ph/0207036](#)] [[INSPIRE](#)].
- [7] G. Isidori and D.M. Straub, *Minimal flavour violation and beyond*, *Eur. Phys. J. C* **72** (2012) 2103 [[arXiv:1202.0464](#)] [[INSPIRE](#)].
- [8] T. Lin, E.W. Kolb and L.-T. Wang, *Probing dark matter couplings to top and bottom quarks at the LHC*, *Phys. Rev. D* **88** (2013) 063510 [[arXiv:1303.6638](#)] [[INSPIRE](#)].

- [9] M.R. Buckley, D. Feld and D. Goncalves, *Scalar simplified models for dark matter*, *Phys. Rev. D* **91** (2015) 015017 [[arXiv:1410.6497](#)] [[INSPIRE](#)].
- [10] U. Haisch and E. Re, *Simplified dark matter top-quark interactions at the LHC*, *JHEP* **06** (2015) 078 [[arXiv:1503.00691](#)] [[INSPIRE](#)].
- [11] U. Haisch, F. Kahlhoefer and J. Unwin, *The impact of heavy-quark loops on LHC dark matter searches*, *JHEP* **07** (2013) 125 [[arXiv:1208.4605](#)] [[INSPIRE](#)].
- [12] CMS collaboration, *Search for the production of dark matter in association with top-quark pairs in the single-lepton final state in proton-proton collisions at $\sqrt{s} = 8$ TeV*, *JHEP* **06** (2015) 121 [[arXiv:1504.03198](#)] [[INSPIRE](#)].
- [13] ATLAS collaboration, *Search for dark matter in events with heavy quarks and missing transverse momentum in pp collisions with the ATLAS detector*, *Eur. Phys. J. C* **75** (2015) 92 [[arXiv:1410.4031](#)] [[INSPIRE](#)].
- [14] CMS collaboration, *Search for dark matter produced in association with heavy-flavor quark pairs in proton-proton collisions at $\sqrt{s} = 13$ TeV*, *Eur. Phys. J. C* **77** (2017) 845 [[arXiv:1706.02581](#)] [[INSPIRE](#)].
- [15] ATLAS collaboration, *Search for dark matter produced in association with bottom or top quarks in $\sqrt{s} = 13$ TeV pp collisions with the ATLAS detector*, *Eur. Phys. J. C* **78** (2018) 18 [[arXiv:1710.11412](#)] [[INSPIRE](#)].
- [16] CMS collaboration, *Search for dark matter particles produced in association with a top quark pair at $\sqrt{s} = 13$ TeV*, *Phys. Rev. Lett.* **122** (2019) 011803 [[arXiv:1807.06522](#)] [[INSPIRE](#)].
- [17] D. Pinna, A. Zucchetta, M.R. Buckley and F. Canelli, *Single top quarks and dark matter*, *Phys. Rev. D* **96** (2017) 035031 [[arXiv:1701.05195](#)] [[INSPIRE](#)].
- [18] U. Haisch, P. Pani and G. Polesello, *Determining the CP nature of spin-0 mediators in associated production of dark matter and $t\bar{t}$ pairs*, *JHEP* **02** (2017) 131 [[arXiv:1611.09841](#)] [[INSPIRE](#)].
- [19] CDF collaboration, *Search for a dark matter candidate produced in association with a single top quark in $p\bar{p}$ collisions at $\sqrt{s} = 1.96$ TeV*, *Phys. Rev. Lett.* **108** (2012) 201802 [[arXiv:1202.5653](#)] [[INSPIRE](#)].
- [20] ATLAS collaboration, *Search for invisible particles produced in association with single-top-quarks in proton-proton collisions at $\sqrt{s} = 8$ TeV with the ATLAS detector*, *Eur. Phys. J. C* **75** (2015) 79 [[arXiv:1410.5404](#)] [[INSPIRE](#)].
- [21] CMS collaboration, *Search for monotop signatures in proton-proton collisions at $\sqrt{s} = 8$ TeV*, *Phys. Rev. Lett.* **114** (2015) 101801 [[arXiv:1410.1149](#)] [[INSPIRE](#)].
- [22] CMS collaboration, *Search for dark matter in events with energetic, hadronically decaying top quarks and missing transverse momentum at $\sqrt{s} = 13$ TeV*, *JHEP* **06** (2018) 027 [[arXiv:1801.08427](#)] [[INSPIRE](#)].
- [23] CMS collaboration, *The CMS experiment at the CERN LHC*, 2008 *JINST* **3** S08004 [[INSPIRE](#)].
- [24] CMS collaboration, *The CMS trigger system*, 2017 *JINST* **12** P01020 [[arXiv:1609.02366](#)] [[INSPIRE](#)].
- [25] CMS collaboration, *Particle-flow reconstruction and global event description with the CMS detector*, 2017 *JINST* **12** P10003 [[arXiv:1706.04965](#)] [[INSPIRE](#)].

- [26] M. Cacciari, G.P. Salam and G. Soyez, *The anti- k_t jet clustering algorithm*, *JHEP* **04** (2008) 063 [[arXiv:0802.1189](#)] [[INSPIRE](#)].
- [27] M. Cacciari, G.P. Salam and G. Soyez, *FastJet user manual*, *Eur. Phys. J. C* **72** (2012) 1896 [[arXiv:1111.6097](#)] [[INSPIRE](#)].
- [28] M. Cacciari, G.P. Salam and G. Soyez, *The catchment area of jets*, *JHEP* **04** (2008) 005 [[arXiv:0802.1188](#)] [[INSPIRE](#)].
- [29] CMS collaboration, *Jet algorithms performance in 13 TeV data*, CMS-PAS-JME-16-003 (2017).
- [30] CMS collaboration, *Identification of heavy-flavour jets with the CMS detector in pp collisions at 13 TeV*, *2018 JINST* **13** P05011 [[arXiv:1712.07158](#)] [[INSPIRE](#)].
- [31] P. Nason, *A new method for combining NLO QCD with shower Monte Carlo algorithms*, *JHEP* **11** (2004) 040 [[hep-ph/0409146](#)] [[INSPIRE](#)].
- [32] S. Frixione, P. Nason and C. Oleari, *Matching NLO QCD computations with parton shower simulations: the POWHEG method*, *JHEP* **11** (2007) 070 [[arXiv:0709.2092](#)] [[INSPIRE](#)].
- [33] S. Alioli, P. Nason, C. Oleari and E. Re, *A general framework for implementing NLO calculations in shower Monte Carlo programs: the POWHEG BOX*, *JHEP* **06** (2010) 043 [[arXiv:1002.2581](#)] [[INSPIRE](#)].
- [34] CMS collaboration, *Measurement of differential cross sections for top quark pair production using the lepton+jets final state in proton-proton collisions at 13 TeV*, *Phys. Rev. D* **95** (2017) 092001 [[arXiv:1610.04191](#)] [[INSPIRE](#)].
- [35] J. Alwall et al., *The automated computation of tree-level and next-to-leading order differential cross sections, and their matching to parton shower simulations*, *JHEP* **07** (2014) 079 [[arXiv:1405.0301](#)] [[INSPIRE](#)].
- [36] M.L. Mangano, M. Moretti, F. Piccinini and M. Treccani, *Matching matrix elements and shower evolution for top-quark production in hadronic collisions*, *JHEP* **01** (2007) 013 [[hep-ph/0611129](#)] [[INSPIRE](#)].
- [37] A. Denner, S. Dittmaier, T. Kasprzik and A. Muck, *Electroweak corrections to $W + jet$ hadroproduction including leptonic W -boson decays*, *JHEP* **08** (2009) 075 [[arXiv:0906.1656](#)] [[INSPIRE](#)].
- [38] A. Denner, S. Dittmaier, T. Kasprzik and A. Muck, *Electroweak corrections to dilepton + jet production at hadron colliders*, *JHEP* **06** (2011) 069 [[arXiv:1103.0914](#)] [[INSPIRE](#)].
- [39] A. Denner, S. Dittmaier, T. Kasprzik and A. Mück, *Electroweak corrections to monojet production at the LHC*, *Eur. Phys. J. C* **73** (2013) 2297 [[arXiv:1211.5078](#)] [[INSPIRE](#)].
- [40] J.H. Kuhn, A. Kulesza, S. Pozzorini and M. Schulze, *Electroweak corrections to hadronic photon production at large transverse momenta*, *JHEP* **03** (2006) 059 [[hep-ph/0508253](#)] [[INSPIRE](#)].
- [41] S. Kallweit et al., *NLO electroweak automation and precise predictions for $W + multijet$ production at the LHC*, *JHEP* **04** (2015) 012 [[arXiv:1412.5157](#)] [[INSPIRE](#)].
- [42] S. Kallweit et al., *NLO QCD+EW predictions for $V + jets$ including off-shell vector-boson decays and multijet merging*, *JHEP* **04** (2016) 021 [[arXiv:1511.08692](#)] [[INSPIRE](#)].
- [43] R. Frederix and S. Frixione, *Merging meets matching in MC@NLO*, *JHEP* **12** (2012) 061 [[arXiv:1209.6215](#)] [[INSPIRE](#)].

- [44] D. Abercrombie et al., *Dark matter benchmark models for early LHC run-2 searches: report of the ATLAS/CMS dark matter forum*, [arXiv:1507.00966](#) [INSPIRE].
- [45] G. Busoni et al., *Recommendations on presenting LHC searches for missing transverse energy signals using simplified s-channel models of dark matter*, [arXiv:1603.04156](#) [INSPIRE].
- [46] A. Albert et al., *Towards the next generation of simplified dark matter models*, *Phys. Dark Univ.* **16** (2017) 49 [[arXiv:1607.06680](#)] [INSPIRE].
- [47] NNPDF collaboration, *Parton distributions for the LHC Run II*, *JHEP* **04** (2015) 040 [[arXiv:1410.8849](#)] [INSPIRE].
- [48] T. Sjöstrand, S. Mrenna and P.Z. Skands, *A brief introduction to PYTHIA 8.1*, *Comput. Phys. Commun.* **178** (2008) 852 [[arXiv:0710.3820](#)] [INSPIRE].
- [49] CMS collaboration, *Event generator tunes obtained from underlying event and multiparton scattering measurements*, *Eur. Phys. J. C* **76** (2016) 155 [[arXiv:1512.00815](#)] [INSPIRE].
- [50] CMS collaboration, *Investigations of the impact of the parton shower tuning in PYTHIA 8 in the modelling of $t\bar{t}$ at $\sqrt{s} = 8$ and 13 TeV*, *CMS-PAS-TOP-16-021* (2016).
- [51] GEANT4 collaboration, *GEANT4 — a simulation toolkit*, *Nucl. Instrum. Meth. A* **506** (2003) 250 [INSPIRE].
- [52] CMS collaboration, *Performance of CMS muon reconstruction in pp collision events at $\sqrt{s} = 7$ TeV*, *2012 JINST* **7** P10002 [[arXiv:1206.4071](#)] [INSPIRE].
- [53] CMS collaboration, *Performance of electron reconstruction and selection with the CMS detector in proton-proton collisions at $\sqrt{s} = 8$ TeV*, *2015 JINST* **10** P06005 [[arXiv:1502.02701](#)] [INSPIRE].
- [54] Y. Bai, H.-C. Cheng, J. Gallicchio and J. Gu, *Stop the top background of the stop search*, *JHEP* **07** (2012) 110 [[arXiv:1203.4813](#)] [INSPIRE].
- [55] CMS collaboration, *Measurement of the inelastic proton-proton cross section at $\sqrt{s} = 13$ TeV*, *JHEP* **07** (2018) 161 [[arXiv:1802.02613](#)] [INSPIRE].
- [56] CMS collaboration, *CMS luminosity measurements for the 2016 data taking period*, *CMS-PAS-LUM-17-001* (2017).
- [57] CMS collaboration, *Jet energy scale and resolution in the CMS experiment in pp collisions at 8 TeV*, *2017 JINST* **12** P02014 [[arXiv:1607.03663](#)] [INSPIRE].
- [58] J. Butterworth et al., *PDF4LHC recommendations for LHC run II*, *J. Phys. G* **43** (2016) 023001 [[arXiv:1510.03865](#)] [INSPIRE].
- [59] CMS collaboration, *Measurements of differential cross sections for associated production of a W boson and jets in proton-proton collisions at $\sqrt{s} = 8$ TeV*, *Phys. Rev. D* **95** (2017) 052002 [[arXiv:1610.04222](#)] [INSPIRE].
- [60] CMS collaboration, *Measurement of the production cross section of a W boson in association with two b jets in pp collisions at $\sqrt{s} = 8$ TeV*, *Eur. Phys. J. C* **77** (2017) 92 [[arXiv:1608.07561](#)] [INSPIRE].
- [61] CMS collaboration, *Measurements of jet multiplicity and differential production cross sections of Z + jets events in proton-proton collisions at $\sqrt{s} = 7$ TeV*, *Phys. Rev. D* **91** (2015) 052008 [[arXiv:1408.3104](#)] [INSPIRE].
- [62] CMS collaboration, *Measurements of the associated production of a Z boson and b jets in pp collisions at $\sqrt{s} = 8$ TeV*, *Eur. Phys. J. C* **77** (2017) 751 [[arXiv:1611.06507](#)] [INSPIRE].

- [63] R.J. Barlow and C. Beeston, *Fitting using finite Monte Carlo samples*, *Comput. Phys. Commun.* **77** (1993) 219 [[INSPIRE](#)].
- [64] L. Moneta et al., *The RooStats project*, *PoS(ACAT2010)057* [[arXiv:1009.1003](#)] [[INSPIRE](#)].
- [65] T. Junk, *Confidence level computation for combining searches with small statistics*, *Nucl. Instrum. Meth. A* **434** (1999) 435.
- [66] A.L. Read, *Presentation of search results: the CL_s technique*, *J. Phys. G* **28** (2002) 2693 [[INSPIRE](#)].
- [67] G. Cowan, K. Cranmer, E. Gross and O. Vitells, *Asymptotic formulae for likelihood-based tests of new physics*, *Eur. Phys. J. C* **71** (2011) 1554 [*Erratum ibid.* **C 73** (2013) 2501] [[arXiv:1007.1727](#)] [[INSPIRE](#)].

The CMS collaboration

Yerevan Physics Institute, Yerevan, Armenia

A.M. Sirunyan, A. Tumasyan

Institut für Hochenergiephysik, Wien, Austria

W. Adam, F. Ambrogio, E. Asilar, T. Bergauer, J. Brandstetter, M. Dragicevic, J. Erö, A. Escalante Del Valle, M. Flechl, R. Frühwirth¹, V.M. Ghete, J. Hrubec, M. Jeitler¹, N. Krammer, I. Krätschmer, D. Liko, T. Madlener, I. Mikulec, N. Rad, H. Rohringer, J. Schieck¹, R. Schöfbeck, M. Spanring, D. Spitzbart, W. Waltenberger, J. Wittmann, C.-E. Wulz¹, M. Zarucki

Institute for Nuclear Problems, Minsk, Belarus

V. Chekhovsky, V. Mossolov, J. Suarez Gonzalez

Universiteit Antwerpen, Antwerpen, Belgium

E.A. De Wolf, D. Di Croce, X. Janssen, J. Lauwers, M. Pieters, H. Van Haevermaet, P. Van Mechelen, N. Van Remortel

Vrije Universiteit Brussel, Brussel, Belgium

S. Abu Zeid, F. Blekman, J. D'Hondt, J. De Clercq, K. Deroover, G. Flouris, D. Lonkowskyi, S. Lowette, I. Marchesini, S. Moortgat, L. Moreels, Q. Python, K. Skovpen, S. Tavernier, W. Van Doninck, P. Van Mulders, I. Van Parijs

Université Libre de Bruxelles, Bruxelles, Belgium

D. Beghin, B. Bilin, H. Brun, B. Clerbaux, G. De Lentdecker, H. Delannoy, B. Dorney, G. Fasanella, L. Favart, R. Goldouzian, A. Grebenyuk, A.K. Kalsi, T. Lenzi, J. Luetic, N. Postiau, E. Starling, L. Thomas, C. Vander Velde, P. Vanlaer, D. Vannerom, Q. Wang

Ghent University, Ghent, Belgium

T. Cornelis, D. Dobur, A. Fagot, M. Gul, I. Khvastunov², D. Poyraz, C. Roskas, D. Trocino, M. Tytgat, W. Verbeke, B. Vermassen, M. Vit, N. Zaganidis

Université Catholique de Louvain, Louvain-la-Neuve, Belgium

H. Bakhshiansohi, O. Bondu, S. Brochet, G. Bruno, C. Caputo, P. David, C. Delaere, M. Delcourt, A. Giammanco, G. Krintiras, V. Lemaitre, A. Magitteri, K. Piotrkowski, A. Saggio, M. Vidal Marono, P. Vischia, S. Wertz, J. Zobec

Centro Brasileiro de Pesquisas Fisicas, Rio de Janeiro, Brazil

F.L. Alves, G.A. Alves, M. Correa Martins Junior, G. Correia Silva, C. Hensel, A. Moraes, M.E. Pol, P. Rebello Teles

Universidade do Estado do Rio de Janeiro, Rio de Janeiro, Brazil

E. Belchior Batista Das Chagas, W. Carvalho, J. Chinellato³, E. Coelho, E.M. Da Costa, G.G. Da Silveira⁴, D. De Jesus Damiao, C. De Oliveira Martins, S. Fonseca De Souza, H. Malbouisson, D. Matos Figueiredo, M. Melo De Almeida, C. Mora Herrera, L. Mundim, H. Nogima, W.L. Prado Da Silva, L.J. Sanchez Rosas, A. Santoro, A. Sznajder, M. Thiel, E.J. Tonelli Manganote³, F. Torres Da Silva De Araujo, A. Vilela Pereira

Universidade Estadual Paulista^a, Universidade Federal do ABC^b, São Paulo, Brazil

S. Ahuja^a, C.A. Bernardes^a, L. Calligaris^a, T.R. Fernandez Perez Tomei^a, E.M. Gregores^b, P.G. Mercadante^b, S.F. Novaes^a, SandraS. Padula^a

Institute for Nuclear Research and Nuclear Energy, Bulgarian Academy of Sciences, Sofia, Bulgaria

A. Aleksandrov, R. Hadjiiska, P. Iaydjiev, A. Marinov, M. Misheva, M. Rodozov, M. Shopova, G. Sultanov

University of Sofia, Sofia, Bulgaria

A. Dimitrov, L. Litov, B. Pavlov, P. Petkov

Beihang University, Beijing, China

W. Fang⁵, X. Gao⁵, L. Yuan

Institute of High Energy Physics, Beijing, China

M. Ahmad, J.G. Bian, G.M. Chen, H.S. Chen, M. Chen, Y. Chen, C.H. Jiang, D. Leggat, H. Liao, Z. Liu, S.M. Shaheen⁶, A. Spiezia, J. Tao, Z. Wang, E. Yazgan, H. Zhang, S. Zhang⁶, J. Zhao

State Key Laboratory of Nuclear Physics and Technology, Peking University, Beijing, China

Y. Ban, G. Chen, A. Levin, J. Li, L. Li, Q. Li, Y. Mao, S.J. Qian, D. Wang

Tsinghua University, Beijing, China

Y. Wang

Universidad de Los Andes, Bogota, Colombia

C. Avila, A. Cabrera, C.A. Carrillo Montoya, L.F. Chaparro Sierra, C. Florez, C.F. González Hernández, M.A. Segura Delgado

University of Split, Faculty of Electrical Engineering, Mechanical Engineering and Naval Architecture, Split, Croatia

B. Courbon, N. Godinovic, D. Lelas, I. Puljak, T. Sculac

University of Split, Faculty of Science, Split, Croatia

Z. Antunovic, M. Kovac

Institute Rudjer Boskovic, Zagreb, Croatia

V. Brigljevic, D. Ferencek, K. Kadija, B. Mesic, A. Starodumov⁷, T. Susa

University of Cyprus, Nicosia, Cyprus

M.W. Ather, A. Attikis, M. Kolosova, G. Mavromanolakis, J. Mousa, C. Nicolaou, F. Ptochos, P.A. Razis, H. Rykaczewski

Charles University, Prague, Czech Republic

M. Finger⁸, M. Finger Jr.⁸

Escuela Politecnica Nacional, Quito, Ecuador

E. Ayala

Universidad San Francisco de Quito, Quito, Ecuador

E. Carrera Jarrin

**Academy of Scientific Research and Technology of the Arab Republic of Egypt,
Egyptian Network of High Energy Physics, Cairo, Egypt**

S. Elgammal⁹, A. Ellithi Kamel¹⁰, E. Salama^{9,11}

National Institute of Chemical Physics and Biophysics, Tallinn, Estonia

S. Bhowmik, A. Carvalho Antunes De Oliveira, R.K. Dewanjee, K. Ehataht, M. Kadastik,
M. Raidal, C. Veelken

Department of Physics, University of Helsinki, Helsinki, Finland

P. Eerola, H. Kirschenmann, J. Pekkanen, M. Voutilainen

Helsinki Institute of Physics, Helsinki, Finland

J. Havukainen, J.K. Heikkilä, T. Järvinen, V. Karimäki, R. Kinnunen, T. Lampén,
K. Lassila-Perini, S. Laurila, S. Lehti, T. Lindén, P. Luukka, T. Mäenpää, H. Siikonen,
E. Tuominen, J. Tuominiemi

Lappeenranta University of Technology, Lappeenranta, Finland

T. Tuuva

IRFU, CEA, Université Paris-Saclay, Gif-sur-Yvette, France

M. Besancon, F. Couderc, M. Dejardin, D. Denegri, J.L. Faure, F. Ferri, S. Ganjour,
A. Givernaud, P. Gras, G. Hamel de Monchenault, P. Jarry, C. Leloup, E. Locci, J. Malcles,
G. Negro, J. Rander, A. Rosowsky, M.Ö. Sahin, M. Titov

**Laboratoire Leprince-Ringuet, Ecole polytechnique, CNRS/IN2P3, Université
Paris-Saclay, Palaiseau, France**

A. Abdulsalam¹², C. Amendola, I. Antropov, F. Beaudette, P. Busson, C. Charlot,
R. Granier de Cassagnac, I. Kucher, A. Lobanov, J. Martin Blanco, C. Martin Perez,
M. Nguyen, C. Ochando, G. Ortona, P. Paganini, P. Pigard, J. Rembser, R. Salerno,
J.B. Sauvan, Y. Sirois, A.G. Stahl Leiton, A. Zabi, A. Zghiche

Université de Strasbourg, CNRS, IPHC UMR 7178, Strasbourg, France

J.-L. Agram¹³, J. Andrea, D. Bloch, J.-M. Brom, E.C. Chabert, V. Cherepanov, C. Collard,
E. Conte¹³, J.-C. Fontaine¹³, D. Gelé, U. Goerlach, M. Jansová, A.-C. Le Bihan, N. Tonon,
P. Van Hove

**Centre de Calcul de l'Institut National de Physique Nucleaire et de Physique
des Particules, CNRS/IN2P3, Villeurbanne, France**

S. Gadrat

Université de Lyon, Université Claude Bernard Lyon 1, CNRS-IN2P3, Institut de Physique Nucléaire de Lyon, Villeurbanne, France

S. Beauceron, C. Bernet, G. Boudoul, N. Chanon, R. Chierici, D. Contardo, P. Depasse, H. El Mamouni, J. Fay, L. Finco, S. Gascon, M. Gouzevitch, G. Grenier, B. Ille, F. Lagarde, I.B. Laktineh, H. Lattaud, M. Lethuillier, L. Mirabito, S. Perries, A. Popov¹⁴, V. Sordini, G. Touquet, M. Vander Donckt, S. Viret

Georgian Technical University, Tbilisi, Georgia

A. Khvedelidze⁸

Tbilisi State University, Tbilisi, Georgia

I. Bagaturia¹⁵

RWTH Aachen University, I. Physikalisches Institut, Aachen, Germany

C. Autermann, L. Feld, M.K. Kiesel, K. Klein, M. Lipinski, M. Preuten, M.P. Rauch, C. Schomakers, J. Schulz, M. Teroerde, B. Wittmer

RWTH Aachen University, III. Physikalisches Institut A, Aachen, Germany

A. Albert, D. Duchardt, M. Erdmann, S. Erdweg, T. Esch, R. Fischer, S. Ghosh, A. Güth, T. Hebbeker, C. Heidemann, K. Hoepfner, H. Keller, L. Mastrolorenzo, M. Merschmeyer, A. Meyer, P. Millet, S. Mukherjee, T. Pook, M. Radziej, H. Reithler, M. Rieger, A. Schmidt, D. Teyssier, S. Thüer

RWTH Aachen University, III. Physikalisches Institut B, Aachen, Germany

G. Flügge, O. Hlushchenko, T. Kress, T. Müller, A. Nehr Korn, A. Nowack, C. Pistone, O. Pooth, D. Roy, H. Sert, A. Stahl¹⁶

Deutsches Elektronen-Synchrotron, Hamburg, Germany

M. Aldaya Martin, T. Arndt, C. Asawatangtrakuldee, I. Babounikau, K. Beernaert, O. Behnke, U. Behrens, A. Bermúdez Martínez, D. Bertsche, A.A. Bin Anuar, K. Borras¹⁷, V. Botta, A. Campbell, P. Connor, C. Contreras-Campana, V. Danilov, A. De Wit, M.M. Defranchis, C. Diez Pardos, D. Domínguez Damiani, G. Eckerlin, T. Eichhorn, A. Elwood, E. Eren, E. Gallo¹⁸, A. Geiser, J.M. Grados Luyando, A. Grohsjean, M. Guthoff, M. Haranko, A. Harb, H. Jung, M. Kasemann, J. Keaveney, C. Kleinwort, J. Knolle, D. Krücker, W. Lange, A. Lelek, T. Lenz, J. Leonard, K. Lipka, W. Lohmann¹⁹, R. Mankel, I.-A. Melzer-Pellmann, A.B. Meyer, M. Meyer, M. Missiroli, J. Mnich, V. Myronenko, S.K. Pflitsch, D. Pitzl, A. Raspereza, P. Saxena, P. Schütze, C. Schwanenberger, R. Shevchenko, A. Singh, H. Tholen, O. Turkot, A. Vagnerini, G.P. Van Onsem, R. Walsh, Y. Wen, K. Wichmann, C. Wissing, O. Zenaiev

University of Hamburg, Hamburg, Germany

R. Aggleton, S. Bein, L. Benato, A. Benecke, V. Blobel, T. Dreyer, A. Ebrahimi, E. Garutti, D. Gonzalez, P. Gunnellini, J. Haller, A. Hinzmann, A. Karavdina, G. Kasieczka, R. Klanner, R. Kogler, N. Kovalchuk, S. Kurz, V. Kutzner, J. Lange, D. Marconi, J. Multhaupt, M. Niedziela, C.E.N. Niemeyer, D. Nowatschin, A. Perieanu, A. Reimers, O. Rieger, C. Scharf, P. Schleper, S. Schumann, J. Schwandt, J. Sonneveld, H. Stadie, G. Steinbrück, F.M. Stober, M. Stöver, B. Vormwald, I. Zoi

Karlsruher Institut fuer Technologie, Karlsruhe, Germany

M. Akbiyik, C. Barth, M. Baselga, S. Baur, E. Butz, R. Caspart, T. Chwalek, F. Colombo, W. De Boer, A. Dierlamm, K. El Morabit, N. Faltermann, B. Freund, M. Giffels, M.A. Harrendorf, F. Hartmann¹⁶, S.M. Heindl, U. Husemann, I. Katkov¹⁴, S. Kudella, S. Mitra, M.U. Mozer, Th. Müller, M. Musich, M. Plagge, G. Quast, K. Rabbertz, M. Schröder, I. Shvetsov, H.J. Simonis, R. Ulrich, S. Wayand, M. Weber, T. Weiler, C. Wöhrmann, R. Wolf

Institute of Nuclear and Particle Physics (INPP), NCSR Demokritos, Aghia Paraskevi, Greece

G. Anagnostou, G. Daskalakis, T. Gerasis, A. Kyriakis, D. Loukas, G. Paspalaki

National and Kapodistrian University of Athens, Athens, Greece

A. Agapitos, G. Karathanasis, P. Kontaxakis, A. Panagiotou, I. Papavergou, N. Saoulidou, E. Tziaferi, K. Vellidis

National Technical University of Athens, Athens, Greece

K. Kousouris, I. Papakrivopoulos, G. Tsipolitis

University of Ioánnina, Ioánnina, Greece

I. Evangelou, C. Foudas, P. Gianneios, P. Katsoulis, P. Kokkas, S. Mallios, N. Manthos, I. Papadopoulos, E. Paradas, J. Strologas, F.A. Triantis, D. Tsitsonis

MTA-ELTE Lendület CMS Particle and Nuclear Physics Group, Eötvös Loránd University, Budapest, Hungary

M. Bartók²⁰, M. Csanad, N. Filipovic, P. Major, M.I. Nagy, G. Pasztor, O. Surányi, G.I. Veres

Wigner Research Centre for Physics, Budapest, Hungary

G. Bencze, C. Hajdu, D. Horvath²¹, Á. Hunyadi, F. Sikler, T.Á. Vámi, V. Veszpremi, G. Vesztergombi[†]

Institute of Nuclear Research ATOMKI, Debrecen, Hungary

N. Beni, S. Czellar, J. Karancki²⁰, A. Makovec, J. Molnar, Z. Szillasi

Institute of Physics, University of Debrecen, Debrecen, Hungary

P. Raics, Z.L. Trocsanyi, B. Ujvari

Indian Institute of Science (IISc), Bangalore, India

S. Choudhury, J.R. Komaragiri, P.C. Tiwari

National Institute of Science Education and Research, HBNI, Bhubaneswar, India

S. Bahinipati²³, C. Kar, P. Mal, K. Mandal, A. Nayak²⁴, S. Roy Chowdhury, D.K. Sahoo²³, S.K. Swain

Panjab University, Chandigarh, India

S. Bansal, S.B. Beri, V. Bhatnagar, S. Chauhan, R. Chawla, N. Dhingra, R. Gupta, A. Kaur, M. Kaur, S. Kaur, P. Kumari, M. Lohan, M. Meena, A. Mehta, K. Sandeep, S. Sharma, J.B. Singh, A.K. Viridi, G. Walia

University of Delhi, Delhi, India

A. Bhardwaj, B.C. Choudhary, R.B. Garg, M. Gola, S. Keshri, Ashok Kumar, S. Malhotra, M. Naimuddin, P. Priyanka, K. Ranjan, Aashaq Shah, R. Sharma

Saha Institute of Nuclear Physics, HBNI, Kolkata, India

R. Bhardwaj²⁵, M. Bharti²⁵, R. Bhattacharya, S. Bhattacharya, U. Bhawandeep²⁵, D. Bhowmik, S. Dey, S. Dutt²⁵, S. Dutta, S. Ghosh, K. Mondal, S. Nandan, A. Purohit, P.K. Rout, A. Roy, G. Saha, S. Sarkar, M. Sharan, B. Singh²⁵, S. Thakur²⁵

Indian Institute of Technology Madras, Madras, India

P.K. Behera, A. Muhammad

Bhabha Atomic Research Centre, Mumbai, India

R. Chudasama, D. Dutta, V. Jha, V. Kumar, D.K. Mishra, P.K. Netrakanti, L.M. Pant, P. Shukla

Tata Institute of Fundamental Research-A, Mumbai, India

T. Aziz, M.A. Bhat, S. Dugad, G.B. Mohanty, N. Sur, B. Sutar, RavindraKumar Verma

Tata Institute of Fundamental Research-B, Mumbai, India

S. Banerjee, S. Bhattacharya, S. Chatterjee, P. Das, M. Guchait, Sa. Jain, S. Karmakar, S. Kumar, M. Maity²⁶, G. Majumder, K. Mazumdar, N. Sahoo, T. Sarkar²⁶

Indian Institute of Science Education and Research (IISER), Pune, India

S. Chauhan, S. Dube, V. Hegde, A. Kapoor, K. Kotheekar, S. Pandey, A. Rane, A. Rastogi, S. Sharma

Institute for Research in Fundamental Sciences (IPM), Tehran, Iran

S. Chenarani²⁷, E. Eskandari Tadavani, S.M. Etesami²⁷, M. Khakzad, M. Mohammadi Najafabadi, M. Naseri, F. Rezaei Hosseinabadi, B. Safarzadeh²⁸, M. Zeinali

University College Dublin, Dublin, Ireland

M. Felcini, M. Grunewald

INFN Sezione di Bari^a, Università di Bari^b, Politecnico di Bari^c, Bari, Italy

M. Abbrescia^{a,b}, C. Calabria^{a,b}, A. Colaleo^a, D. Creanza^{a,c}, L. Cristella^{a,b}, N. De Filippis^{a,c}, M. De Palma^{a,b}, A. Di Florio^{a,b}, F. Errico^{a,b}, L. Fiore^a, A. Gelmi^{a,b}, G. Iaselli^{a,c}, M. Ince^{a,b}, S. Lezki^{a,b}, G. Maggi^{a,c}, M. Maggi^a, G. Miniello^{a,b}, S. My^{a,b}, S. Nuzzo^{a,b}, A. Pompili^{a,b}, G. Pugliese^{a,c}, R. Radogna^a, A. Ranieri^a, G. Selvaggi^{a,b}, A. Sharma^a, L. Silvestris^a, R. Venditti^a, P. Verwilligen^a

INFN Sezione di Bologna^a, Università di Bologna^b, Bologna, Italy

G. Abbiendi^a, C. Battilana^{a,b}, D. Bonacorsi^{a,b}, L. Borgonovi^{a,b}, S. Braibant-Giacomelli^{a,b}, R. Campanini^{a,b}, P. Capiluppi^{a,b}, A. Castro^{a,b}, F.R. Cavallo^a, S.S. Chhibra^{a,b},

G. Codispoti^{a,b}, M. Cuffiani^{a,b}, G.M. Dallavalle^a, F. Fabbri^a, A. Fanfani^{a,b}, E. Fontanesi, P. Giacomelli^a, C. Grandi^a, L. Guiducci^{a,b}, F. Iemmi^{a,b}, S. Lo Meo^a, S. Marcellini^a, G. Masetti^a, A. Montanari^a, F.L. Navarria^{a,b}, A. Perrotta^a, F. Primavera^{a,b,16}, A.M. Rossi^{a,b}, T. Rovelli^{a,b}, G.P. Siroli^{a,b}, N. Tosi^a

INFN Sezione di Catania^a, Università di Catania^b, Catania, Italy

S. Albergo^{a,b}, A. Di Mattia^a, R. Potenza^{a,b}, A. Tricomi^{a,b}, C. Tuve^{a,b}

INFN Sezione di Firenze^a, Università di Firenze^b, Firenze, Italy

G. Barbagli^a, K. Chatterjee^{a,b}, V. Ciulli^{a,b}, C. Civinini^a, R. D'Alessandro^{a,b}, E. Focardi^{a,b}, G. Latino, P. Lenzi^{a,b}, M. Meschini^a, S. Paoletti^a, L. Russo^{a,29}, G. Sguazzoni^a, D. Strom^a, L. Viliani^a

INFN Laboratori Nazionali di Frascati, Frascati, Italy

L. Benussi, S. Bianco, F. Fabbri, D. Piccolo

INFN Sezione di Genova^a, Università di Genova^b, Genova, Italy

F. Ferro^a, R. Mulargia^{a,b}, F. Ravera^{a,b}, E. Robutti^a, S. Tosi^{a,b}

INFN Sezione di Milano-Bicocca^a, Università di Milano-Bicocca^b, Milano, Italy

A. Benaglia^a, A. Beschi^b, F. Brivio^{a,b}, V. Ciriolo^{a,b,16}, S. Di Guida^{a,b,16}, M.E. Dinardo^{a,b}, S. Fiorendi^{a,b}, S. Gennai^a, A. Ghezzi^{a,b}, P. Govoni^{a,b}, M. Malberti^{a,b}, S. Malvezzi^a, D. Menasce^a, F. Monti, L. Moroni^a, M. Paganoni^{a,b}, D. Pedrini^a, S. Ragazzi^{a,b}, T. Tabarelli de Fatis^{a,b}, D. Zuolo^{a,b}

INFN Sezione di Napoli^a, Università di Napoli 'Federico II'^b, Napoli, Italy, Università della Basilicata^c, Potenza, Italy, Università G. Marconi^d, Roma, Italy

S. Buontempo^a, N. Cavallo^{a,c}, A. De Iorio^{a,b}, A. Di Crescenzo^{a,b}, F. Fabozzi^{a,c}, F. Fienga^a, G. Galati^a, A.O.M. Iorio^{a,b}, W.A. Khan^a, L. Lista^a, S. Meola^{a,d,16}, P. Paolucci^{a,16}, C. Sciacca^{a,b}, E. Voevodina^{a,b}

INFN Sezione di Padova^a, Università di Padova^b, Padova, Italy, Università di Trento^c, Trento, Italy

P. Azzi^a, N. Bacchetta^a, D. Bisello^{a,b}, A. Boletti^{a,b}, A. Bragagnolo, R. Carlin^{a,b}, P. Checchia^a, M. Dall'Osso^{a,b}, P. De Castro Manzano^a, T. Dorigo^a, U. Dosselli^a, F. Gasparini^{a,b}, U. Gasparini^{a,b}, A. Gozzelino^a, S.Y. Hoh, S. Lacaprara^a, P. Lujan, M. Margoni^{a,b}, A.T. Meneguzzo^{a,b}, J. Pazzini^{a,b}, M. Presilla^b, P. Ronchese^{a,b}, R. Rossin^{a,b}, F. Simonetto^{a,b}, A. Tiko, E. Torassa^a, M. Tosi^{a,b}, M. Zanetti^{a,b}, P. Zotto^{a,b}, G. Zumerle^{a,b}

INFN Sezione di Pavia^a, Università di Pavia^b, Pavia, Italy

A. Braghieri^a, A. Magnani^a, P. Montagna^{a,b}, S.P. Ratti^{a,b}, V. Re^a, M. Ressegotti^{a,b}, C. Riccardi^{a,b}, P. Salvini^a, I. Vai^{a,b}, P. Vitulo^{a,b}

INFN Sezione di Perugia^a, Università di Perugia^b, Perugia, Italy

M. Biasini^{a,b}, G.M. Bilei^a, C. Cecchi^{a,b}, D. Ciangottini^{a,b}, L. Fanò^{a,b}, P. Lariccia^{a,b}, R. Leonardi^{a,b}, E. Manoni^a, G. Mantovani^{a,b}, V. Mariani^{a,b}, M. Menichelli^a, A. Rossi^{a,b}, A. Santocchia^{a,b}, D. Spiga^a

INFN Sezione di Pisa^a, Università di Pisa^b, Scuola Normale Superiore di Pisa^c, Pisa, Italy

K. Androsov^a, P. Azzurri^a, G. Bagliesi^a, L. Bianchini^a, T. Boccali^a, L. Borrello, R. Castaldi^a, M.A. Ciocci^{a,b}, R. Dell’Orso^a, G. Fedi^a, F. Fiori^{a,c}, L. Giannini^{a,c}, A. Giassi^a, M.T. Grippo^a, F. Ligabue^{a,c}, E. Manca^{a,c}, G. Mandorli^{a,c}, A. Messineo^{a,b}, F. Palla^a, A. Rizzi^{a,b}, G. Rolandi³⁰, P. Spagnolo^a, R. Tenchini^a, G. Tonelli^{a,b}, A. Venturi^a, P.G. Verdini^a

INFN Sezione di Roma^a, Sapienza Università di Roma^b, Rome, Italy

L. Barone^{a,b}, F. Cavallari^a, M. Cipriani^{a,b}, D. Del Re^{a,b}, E. Di Marco^{a,b}, M. Diemoz^a, S. Gelli^{a,b}, E. Longo^{a,b}, B. Marzocchi^{a,b}, P. Meridiani^a, G. Organtini^{a,b}, F. Pandolfi^a, R. Paramatti^{a,b}, F. Preiato^{a,b}, S. Rahatlou^{a,b}, C. Rovelli^a, F. Santanastasio^{a,b}

INFN Sezione di Torino^a, Università di Torino^b, Torino, Italy, Università del Piemonte Orientale^c, Novara, Italy

N. Amapane^{a,b}, R. Arcidiacono^{a,c}, S. Argiro^{a,b}, M. Arneodo^{a,c}, N. Bartosik^a, R. Bellan^{a,b}, C. Biino^a, A. Cappati^{a,b}, N. Cartiglia^a, F. Cenna^{a,b}, S. Cometti^a, M. Costa^{a,b}, R. Covarelli^{a,b}, N. Demaria^a, B. Kiani^{a,b}, C. Mariotti^a, S. Maselli^a, E. Migliore^{a,b}, V. Monaco^{a,b}, E. Monteil^{a,b}, M. Monteno^a, M.M. Obertino^{a,b}, L. Pacher^{a,b}, N. Pastrone^a, M. Pelliccioni^a, G.L. Pinna Angioni^{a,b}, A. Romero^{a,b}, M. Ruspa^{a,c}, R. Sacchi^{a,b}, R. Salvatico^{a,b}, K. Shchelina^{a,b}, V. Sola^a, A. Solano^{a,b}, D. Soldi^{a,b}, A. Staiano^a

INFN Sezione di Trieste^a, Università di Trieste^b, Trieste, Italy

S. Belforte^a, V. Candelise^{a,b}, M. Casarsa^a, F. Cossutti^a, A. Da Rold^{a,b}, G. Della Ricca^{a,b}, F. Vazzoler^{a,b}, A. Zanetti^a

Kyungpook National University, Daegu, Korea

D.H. Kim, G.N. Kim, M.S. Kim, J. Lee, S. Lee, S.W. Lee, C.S. Moon, Y.D. Oh, S.I. Pak, S. Sekmen, D.C. Son, Y.C. Yang

Chonnam National University, Institute for Universe and Elementary Particles, Kwangju, Korea

H. Kim, D.H. Moon, G. Oh

Hanyang University, Seoul, Korea

B. Francois, J. Goh³¹, T.J. Kim

Korea University, Seoul, Korea

S. Cho, S. Choi, Y. Go, D. Gyun, S. Ha, B. Hong, Y. Jo, K. Lee, K.S. Lee, S. Lee, J. Lim, S.K. Park, Y. Roh

Sejong University, Seoul, Korea

H.S. Kim

Seoul National University, Seoul, Korea

J. Almond, J. Kim, J.S. Kim, H. Lee, K. Lee, K. Nam, S.B. Oh, B.C. Radburn-Smith, S.h. Seo, U.K. Yang, H.D. Yoo, G.B. Yu

University of Seoul, Seoul, Korea

D. Jeon, H. Kim, J.H. Kim, J.S.H. Lee, I.C. Park

Sungkyunkwan University, Suwon, Korea

Y. Choi, C. Hwang, J. Lee, I. Yu

Vilnius University, Vilnius, Lithuania

V. Dudenas, A. Juodagalvis, J. Vaitkus

National Centre for Particle Physics, Universiti Malaya, Kuala Lumpur, MalaysiaI. Ahmed, Z.A. Ibrahim, M.A.B. Md Ali³², F. Mohamad Idris³³, W.A.T. Wan Abdullah, M.N. Yusli, Z. Zolkapli**Universidad de Sonora (UNISON), Hermosillo, Mexico**

J.F. Benitez, A. Castaneda Hernandez, J.A. Murillo Quijada

Centro de Investigacion y de Estudios Avanzados del IPN, Mexico City, MexicoH. Castilla-Valdez, E. De La Cruz-Burelo, M.C. Duran-Osuna, I. Heredia-De La Cruz³⁴, R. Lopez-Fernandez, J. Mejia Guisao, R.I. Rabadan-Trejo, M. Ramirez-Garcia, G. Ramirez-Sanchez, R. Reyes-Almanza, A. Sanchez-Hernandez**Universidad Iberoamericana, Mexico City, Mexico**

S. Carrillo Moreno, C. Oropeza Barrera, F. Vazquez Valencia

Benemerita Universidad Autonoma de Puebla, Puebla, Mexico

J. Eysermans, I. Pedraza, H.A. Salazar Ibarquen, C. Uribe Estrada

Universidad Autónoma de San Luis Potosí, San Luis Potosí, Mexico

A. Morelos Pineda

University of Auckland, Auckland, New Zealand

D. Krofcheck

University of Canterbury, Christchurch, New Zealand

S. Bheesette, P.H. Butler

National Centre for Physics, Quaid-I-Azam University, Islamabad, Pakistan

A. Ahmad, M. Ahmad, M.I. Asghar, Q. Hassan, H.R. Hoorani, A. Saddique, M.A. Shah, M. Shoaib, M. Waqas

National Centre for Nuclear Research, Swierk, Poland

H. Bialkowska, M. Bluj, B. Boimska, T. Frueboes, M. Górski, M. Kazana, M. Szleper, P. Traczyk, P. Zalewski

Institute of Experimental Physics, Faculty of Physics, University of Warsaw, Warsaw, PolandK. Bunkowski, A. Byszuk³⁵, K. Doroba, A. Kalinowski, M. Konecki, J. Krolikowski, M. Misiura, M. Olszewski, A. Pyskir, M. Walczak

Laboratório de Instrumentação e Física Experimental de Partículas, Lisboa, Portugal

M. Araujo, P. Bargassa, C. Beirão Da Cruz E Silva, A. Di Francesco, P. Faccioli, B. Galinhas, M. Gallinaro, J. Hollar, N. Leonardo, J. Seixas, G. Strong, O. Toldaiev, J. Varela

Joint Institute for Nuclear Research, Dubna, Russia

S. Afanasiev, P. Bunin, M. Gavrilenko, I. Golutvin, I. Gorbunov, A. Kamenev, V. Karjavine, A. Lanev, A. Malakhov, V. Matveev^{36,37}, P. Moisezenz, V. Palichik, V. Perelygin, S. Shmatov, S. Shulha, N. Skatchkov, V. Smirnov, N. Voytishin, A. Zarubin

Petersburg Nuclear Physics Institute, Gatchina (St. Petersburg), Russia

V. Golovtsov, Y. Ivanov, V. Kim³⁸, E. Kuznetsova³⁹, P. Levchenko, V. Murzin, V. Oreshkin, I. Smirnov, D. Sosnov, V. Sulimov, L. Uvarov, S. Vavilov, A. Vorobyev

Institute for Nuclear Research, Moscow, Russia

Yu. Andreev, A. Dermenev, S. Gninenko, N. Golubev, A. Karneyeu, M. Kirsanov, N. Krasnikov, A. Pashenkov, D. Tlisov, A. Toropin

Institute for Theoretical and Experimental Physics, Moscow, Russia

V. Epshteyn, V. Gavrilov, N. Lychkovskaya, V. Popov, I. Pozdnyakov, G. Safronov, A. Spiridonov, A. Stepenov, V. Stolin, M. Toms, E. Vlasov, A. Zhokin

Moscow Institute of Physics and Technology, Moscow, Russia

T. Aushev

National Research Nuclear University ‘Moscow Engineering Physics Institute’ (MEPhI), Moscow, Russia

R. Chistov⁴⁰, M. Danilov⁴⁰, P. Parygin, D. Philippov, S. Polikarpov⁴⁰, E. Tarkovskii

P.N. Lebedev Physical Institute, Moscow, Russia

V. Andreev, M. Azarkin, I. Dremin³⁷, M. Kirakosyan, A. Terkulov

Skobeltsyn Institute of Nuclear Physics, Lomonosov Moscow State University, Moscow, Russia

A. Baskakov, A. Belyaev, E. Boos, V. Bunichev, M. Dubinin⁴¹, L. Dudko, A. Ershov, V. Klyukhin, N. Korneeva, I. Lokhtin, I. Miagkov, S. Obraztsov, M. Perfilov, V. Savrin, P. Volkov

Novosibirsk State University (NSU), Novosibirsk, Russia

A. Barnyakov⁴², V. Blinov⁴², T. Dimova⁴², L. Kardapoltsev⁴², Y. Skovpen⁴²

Institute for High Energy Physics of National Research Centre ‘Kurchatov Institute’, Protvino, Russia

I. Azhgirey, I. Bayshev, S. Bitioukov, V. Kachanov, A. Kalinin, D. Konstantinov, P. Mandrik, V. Petrov, R. Ryutin, S. Slabospitskii, A. Sobol, S. Troshin, N. Tyurin, A. Uzunian, A. Volkov

National Research Tomsk Polytechnic University, Tomsk, Russia

A. Babaev, S. Baidali, V. Okhotnikov

University of Belgrade, Faculty of Physics and Vinca Institute of Nuclear Sciences, Belgrade, SerbiaP. Adzic⁴³, P. Cirkovic, D. Devetak, M. Dordevic, J. Milosevic**Centro de Investigaciones Energéticas Medioambientales y Tecnológicas (CIEMAT), Madrid, Spain**

J. Alcaraz Maestre, A. Álvarez Fernández, I. Bachiller, M. Barrio Luna, J.A. Brochero Cifuentes, M. Cerrada, N. Colino, B. De La Cruz, A. Delgado Peris, C. Fernandez Bedoya, J.P. Fernández Ramos, J. Flix, M.C. Fouz, O. Gonzalez Lopez, S. Goy Lopez, J.M. Hernandez, M.I. Josa, D. Moran, A. Pérez-Calero Yzquierdo, J. Puerta Pelayo, I. Redondo, L. Romero, S. Sánchez Navas, M.S. Soares, A. Triossi

Universidad Autónoma de Madrid, Madrid, Spain

C. Albajar, J.F. de Trocóniz

Universidad de Oviedo, Oviedo, Spain

J. Cuevas, C. Erice, J. Fernandez Menendez, S. Folgueras, I. Gonzalez Caballero, J.R. González Fernández, E. Palencia Cortezon, V. Rodríguez Bouza, S. Sanchez Cruz, J.M. Vizan Garcia

Instituto de Física de Cantabria (IFCA), CSIC-Universidad de Cantabria, Santander, Spain

I.J. Cabrillo, A. Calderon, B. Chazin Quero, J. Duarte Campderros, M. Fernandez, P.J. Fernández Manteca, A. García Alonso, J. Garcia-Ferrero, G. Gomez, A. Lopez Virto, J. Marco, C. Martinez Rivero, P. Martinez Ruiz del Arbol, F. Matorras, J. Piedra Gomez, C. Prieels, T. Rodrigo, A. Ruiz-Jimeno, L. Scodellaro, N. Trevisani, I. Vila, R. Villar Cortabitarte

University of Ruhuna, Department of Physics, Matara, Sri Lanka

N. Wickramage

CERN, European Organization for Nuclear Research, Geneva, SwitzerlandD. Abbaneo, B. Akgun, E. Auffray, G. Auzinger, P. Baillon, A.H. Ball, D. Barney, J. Bendavid, M. Bianco, A. Bocci, C. Botta, E. Brondolin, T. Camporesi, M. Cepeda, G. Cerminara, E. Chapon, Y. Chen, G. Cucciati, D. d'Enterria, A. Dabrowski, N. Daci, V. Daponte, A. David, A. De Roeck, N. Deelen, M. Dobson, M. Dünser, N. Dupont, A. Elliott-Peisert, P. Everaerts, F. Fallavollita⁴⁴, D. Fasanella, G. Franzoni, J. Fulcher, W. Funk, D. Gigi, A. Gilbert, K. Gill, F. Glege, M. Gruchala, M. Guilbaud, D. Gulhan, J. Hegeman, C. Heidegger, V. Innocente, A. Jafari, P. Janot, O. Karacheban¹⁹, J. Kieseler, A. Kornmayer, M. Krammer¹, C. Lange, P. Lecoq, C. Lourenço, L. Malgeri, M. Mannelli, A. Massironi, F. Meijers, J.A. Merlin, S. Mersi, E. Meschi, P. Milenovic⁴⁵, F. Moortgat, M. Mulders, J. Ngadiuba, S. Nourbakhsh, S. Orfanelli, L. Orsini, F. Pantaleo¹⁶, L. Pape, E. Perez, M. Peruzzi, A. Petrilli, G. Petrucciani, A. Pfeiffer, M. Pierini, F.M. Pitters, D. Rabady, A. Racz, T. Reis, M. Rovere, H. Sakulin, C. Schäfer, C. Schwick, M. Selvaggi,

A. Sharma, P. Silva, P. Sphicas⁴⁶, A. Stakia, J. Steggemann, D. Treille, A. Tsirou, V. Veckalns⁴⁷, M. Verzetti, W.D. Zeuner

Paul Scherrer Institut, Villigen, Switzerland

L. Caminada⁴⁸, K. Deiters, W. Erdmann, R. Horisberger, Q. Ingram, H.C. Kaestli, D. Kotlinski, U. Langenegger, T. Rohe, S.A. Wiederkehr

ETH Zurich — Institute for Particle Physics and Astrophysics (IPA), Zurich, Switzerland

M. Backhaus, L. Bäni, P. Berger, N. Chernyavskaya, G. Dissertori, M. Dittmar, M. Donegà, C. Dorfer, T.A. Gómez Espinosa, C. Grab, D. Hits, T. Klijsma, W. Lustermann, R.A. Manzoni, M. Marionneau, M.T. Meinhard, F. Micheli, P. Musella, F. Nessi-Tedaldi, J. Pata, F. Pauss, G. Perrin, L. Perrozzi, S. Pigazzini, M. Quittnat, C. Reissel, D. Ruini, D.A. Sanz Becerra, M. Schönenberger, L. Shchutska, V.R. Tavolaro, K. Theofilatos, M.L. Vesterbacka Olsson, R. Wallny, D.H. Zhu

Universität Zürich, Zurich, Switzerland

T.K. Aarrestad, C. AMSler⁴⁹, D. Brzhechko, M.F. Canelli, A. De Cosa, R. Del Burgo, S. Donato, C. Galloni, T. Hreus, B. Kilminster, S. Leontsinis, I. Neutelings, G. Rauco, P. Robmann, D. Salerno, K. Schweiger, C. Seitz, Y. Takahashi, A. Zucchetta

National Central University, Chung-Li, Taiwan

T.H. Doan, R. Khurana, C.M. Kuo, W. Lin, A. Pozdnyakov, S.S. Yu

National Taiwan University (NTU), Taipei, Taiwan

P. Chang, Y. Chao, K.F. Chen, P.H. Chen, W.-S. Hou, Y.F. Liu, R.-S. Lu, E. Paganis, A. Psallidas, A. Steen

Chulalongkorn University, Faculty of Science, Department of Physics, Bangkok, Thailand

B. Asavapibhop, N. Srimanobhas, N. Suwonjandee

Çukurova University, Physics Department, Science and Art Faculty, Adana, Turkey

A. Bat, F. Boran, S. Cerci⁵⁰, S. Damarseckin, Z.S. Demiroglu, F. Dolek, C. Dozen, I. Dumanoglu, S. Girgis, G. Gokbulut, Y. Guler, E. Gurpinar, I. Hos⁵¹, C. Isik, E.E. Kangal⁵², O. Kara, A. Kayis Topaksu, U. Kiminsu, M. Oglakci, G. Onengut, K. Ozdemir⁵³, S. Ozturk⁵⁴, D. Sunar Cerci⁵⁰, B. Tali⁵⁰, U.G. Tok, S. Turkcapar, I.S. Zorbakir, C. Zorbilmez

Middle East Technical University, Physics Department, Ankara, Turkey

B. Isildak⁵⁵, G. Karapinar⁵⁶, M. Yalvac, M. Zeyrek

Bogazici University, Istanbul, Turkey

I.O. Atakisi, E. Gülmez, M. Kaya⁵⁷, O. Kaya⁵⁸, S. Ozkorucuklu⁵⁹, S. Tekten, E.A. Yetkin⁶⁰

Istanbul Technical University, Istanbul, Turkey

M.N. Agaras, A. Cakir, K. Cankocak, Y. Komurcu, S. Sen⁶¹

**Institute for Scintillation Materials of National Academy of Science of Ukraine,
Kharkov, Ukraine**

B. Grynyov

**National Scientific Center, Kharkov Institute of Physics and Technology,
Kharkov, Ukraine**

L. Levchuk

University of Bristol, Bristol, United Kingdom

F. Ball, J.J. Brooke, D. Burns, E. Clement, D. Cussans, O. Davignon, H. Flacher, J. Goldstein, G.P. Heath, H.F. Heath, L. Kreczko, D.M. Newbold⁶², S. Paramesvaran, B. Penning, T. Sakuma, D. Smith, V.J. Smith, J. Taylor, A. Titterton

Rutherford Appleton Laboratory, Didcot, United Kingdom

K.W. Bell, A. Belyaev⁶³, C. Brew, R.M. Brown, D. Cieri, D.J.A. Cockerill, J.A. Coughlan, K. Harder, S. Harper, J. Linacre, K. Manolopoulos, E. Olaiya, D. Petyt, C.H. Shepherd-Themistocleous, A. Thea, I.R. Tomalin, T. Williams, W.J. Womersley

Imperial College, London, United Kingdom

R. Bainbridge, P. Bloch, J. Borg, S. Breeze, O. Buchmuller, A. Bundock, D. Colling, P. Dauncey, G. Davies, M. Della Negra, R. Di Maria, G. Hall, G. Iles, T. James, M. Komm, C. Laner, L. Lyons, A.-M. Magnan, S. Malik, A. Martelli, J. Nash⁶⁴, A. Nikitenko⁷, V. Palladino, M. Pesaresi, D.M. Raymond, A. Richards, A. Rose, E. Scott, C. Seez, A. Shtipliyski, G. Singh, M. Stoye, T. Strebler, S. Summers, A. Tapper, K. Uchida, T. Virdee¹⁶, N. Wardle, D. Winterbottom, J. Wright, S.C. Zenz

Brunel University, Uxbridge, United Kingdom

J.E. Cole, P.R. Hobson, A. Khan, P. Kyberd, C.K. Mackay, A. Morton, I.D. Reid, L. Teodorescu, S. Zahid

Baylor University, Waco, U.S.A.

K. Call, J. Dittmann, K. Hatakeyama, H. Liu, C. Madrid, B. McMaster, N. Pastika, C. Smith

Catholic University of America, Washington, DC, U.S.A.

R. Bartek, A. Dominguez

The University of Alabama, Tuscaloosa, U.S.A.

A. Buccilli, S.I. Cooper, C. Henderson, P. Rumerio, C. West

Boston University, Boston, U.S.A.

D. Arcaro, T. Bose, D. Gastler, D. Pinna, D. Rankin, C. Richardson, J. Rohlf, L. Sulak, D. Zou

Brown University, Providence, U.S.A.

G. Benelli, X. Coubez, D. Cutts, M. Hadley, J. Hakala, U. Heintz, J.M. Hogan⁶⁵, K.H.M. Kwok, E. Laird, G. Landsberg, J. Lee, Z. Mao, M. Narain, S. Sagir⁶⁶, R. Syarif, E. Usai, D. Yu

University of California, Davis, Davis, U.S.A.

R. Band, C. Brainerd, R. Breedon, D. Burns, M. Calderon De La Barca Sanchez, M. Chertok, J. Conway, R. Conway, P.T. Cox, R. Erbacher, C. Flores, G. Funk, W. Ko, O. Kukral, R. Lander, M. Mulhearn, D. Pellett, J. Pilot, S. Shalhout, M. Shi, D. Stolp, D. Taylor, K. Tos, M. Tripathi, Z. Wang, F. Zhang

University of California, Los Angeles, U.S.A.

M. Bachtis, C. Bravo, R. Cousins, A. Dasgupta, A. Florent, J. Hauser, M. Ignatenko, N. Mccoll, S. Regnard, D. Saltzberg, C. Schnaible, V. Valuev

University of California, Riverside, Riverside, U.S.A.

E. Bouvier, K. Burt, R. Clare, J.W. Gary, S.M.A. Ghiasi Shirazi, G. Hanson, G. Karapostoli, E. Kennedy, F. Lacroix, O.R. Long, M. Olmedo Negrete, M.I. Paneva, W. Si, L. Wang, H. Wei, S. Wimpenny, B.R. Yates

University of California, San Diego, La Jolla, U.S.A.

J.G. Branson, P. Chang, S. Cittolin, M. Derdzinski, R. Gerosa, D. Gilbert, B. Hashemi, A. Holzner, D. Klein, G. Kole, V. Krutelyov, J. Letts, M. Masciovecchio, D. Olivito, S. Padhi, M. Pieri, M. Sani, V. Sharma, S. Simon, M. Tadel, A. Vartak, S. Wasserbaech⁶⁷, J. Wood, F. Würthwein, A. Yagil, G. Zevi Della Porta

University of California, Santa Barbara — Department of Physics, Santa Barbara, U.S.A.

N. Amin, R. Bhandari, C. Campagnari, M. Citron, V. Dutta, M. Franco Sevilla, L. Gouskos, R. Heller, J. Incandela, H. Mei, A. Ovcharova, H. Qu, J. Richman, D. Stuart, I. Suarez, S. Wang, J. Yoo

California Institute of Technology, Pasadena, U.S.A.

D. Anderson, A. Bornheim, J.M. Lawhorn, N. Lu, H.B. Newman, T.Q. Nguyen, M. Spiropulu, J.R. Vlimant, R. Wilkinson, S. Xie, Z. Zhang, R.Y. Zhu

Carnegie Mellon University, Pittsburgh, U.S.A.

M.B. Andrews, T. Ferguson, T. Mudholkar, M. Paulini, M. Sun, I. Vorobiev, M. Weinberg

University of Colorado Boulder, Boulder, U.S.A.

J.P. Cumalat, W.T. Ford, F. Jensen, A. Johnson, E. MacDonald, T. Mulholland, R. Patel, A. Perloff, K. Stenson, K.A. Ulmer, S.R. Wagner

Cornell University, Ithaca, U.S.A.

J. Alexander, J. Chaves, Y. Cheng, J. Chu, A. Datta, K. Mcdermott, N. Mirman, J.R. Patterson, D. Quach, A. Rinkevicius, A. Ryd, L. Skinnari, L. Soffi, S.M. Tan, Z. Tao, J. Thom, J. Tucker, P. Wittich, M. Zientek

Fermi National Accelerator Laboratory, Batavia, U.S.A.

S. Abdullin, M. Albrow, M. Alyari, G. Apollinari, A. Apresyan, A. Apyan, S. Banerjee, L.A.T. Bauerdick, A. Beretvas, J. Berryhill, P.C. Bhat, K. Burkett, J.N. Butler, A. Canepa, G.B. Cerati, H.W.K. Cheung, F. Chlebana, M. Cremonesi, J. Duarte, V.D. Elvira, J. Freeman, Z. Gecse, E. Gottschalk, L. Gray, D. Green, S. Grünendahl, O. Gutsche,

J. Hanlon, R.M. Harris, S. Hasegawa, J. Hirschauer, Z. Hu, B. Jayatilaka, S. Jindariani, M. Johnson, U. Joshi, B. Klima, M.J. Kortelainen, B. Kreis, S. Lammel, D. Lincoln, R. Lipton, M. Liu, T. Liu, J. Lykken, K. Maeshima, J.M. Marraffino, D. Mason, P. McBride, P. Merkel, S. Mrenna, S. Nahn, V. O'Dell, K. Pedro, C. Pena, O. Prokofyev, G. Rakness, L. Ristori, A. Savoy-Navarro⁶⁸, B. Schneider, E. Sexton-Kennedy, A. Soha, W.J. Spalding, L. Spiegel, S. Stoynev, J. Strait, N. Strobbe, L. Taylor, S. Tkaczyk, N.V. Tran, L. Uplegger, E.W. Vaandering, C. Vernieri, M. Verzocchi, R. Vidal, M. Wang, H.A. Weber, A. Whitbeck

University of Florida, Gainesville, U.S.A.

D. Acosta, P. Avery, P. Bortignon, D. Bourilkov, A. Brinkerhoff, L. Cadamuro, A. Carnes, D. Curry, R.D. Field, S.V. Gleyzer, B.M. Joshi, J. Konigsberg, A. Korytov, K.H. Lo, P. Ma, K. Matchev, G. Mitselmakher, D. Rosenzweig, K. Shi, D. Sperka, J. Wang, S. Wang, X. Zuo

Florida International University, Miami, U.S.A.

Y.R. Joshi, S. Linn

Florida State University, Tallahassee, U.S.A.

A. Ackert, T. Adams, A. Askew, S. Hagopian, V. Hagopian, K.F. Johnson, T. Kolberg, G. Martinez, T. Perry, H. Prosper, A. Saha, C. Schiber, R. Yohay

Florida Institute of Technology, Melbourne, U.S.A.

M.M. Baarmand, V. Bhopatkar, S. Colafranceschi, M. Hohlmann, D. Noonan, M. Rahmani, T. Roy, F. Yumiceva

University of Illinois at Chicago (UIC), Chicago, U.S.A.

M.R. Adams, L. Apanasevich, D. Berry, R.R. Betts, R. Cavanaugh, X. Chen, S. Dittmer, O. Evdokimov, C.E. Gerber, D.A. Hangal, D.J. Hofman, K. Jung, J. Kamin, C. Mills, M.B. Tonjes, N. Varelas, H. Wang, X. Wang, Z. Wu, J. Zhang

The University of Iowa, Iowa City, U.S.A.

M. Alhusseini, B. Bilki⁶⁹, W. Clarida, K. Dilsiz⁷⁰, S. Durgut, R.P. Gandrajula, M. Haytmyradov, V. Khristenko, J.-P. Merlo, A. Mestvirishvili, A. Moeller, J. Nachtman, H. Ogul⁷¹, Y. Onel, F. Ozok⁷², A. Penzo, C. Snyder, E. Tiras, J. Wetzel

Johns Hopkins University, Baltimore, U.S.A.

B. Blumenfeld, A. Cocoros, N. Eminizer, D. Fehling, L. Feng, A.V. Gritsan, W.T. Hung, P. Maksimovic, J. Roskes, U. Sarica, M. Swartz, M. Xiao, C. You

The University of Kansas, Lawrence, U.S.A.

A. Al-bataineh, P. Baringer, A. Bean, S. Boren, J. Bowen, A. Bylinkin, J. Castle, S. Khalil, A. Kropivnitskaya, D. Majumder, W. Mcbrayer, M. Murray, C. Rogan, S. Sanders, E. Schmitz, J.D. Tapia Takaki, Q. Wang

Kansas State University, Manhattan, U.S.A.

S. Duric, A. Ivanov, K. Kaadze, D. Kim, Y. Maravin, D.R. Mendis, T. Mitchell, A. Modak, A. Mohammadi

Lawrence Livermore National Laboratory, Livermore, U.S.A.

F. Rebassoo, D. Wright

University of Maryland, College Park, U.S.A.

A. Baden, O. Baron, A. Belloni, S.C. Eno, Y. Feng, C. Ferraioli, N.J. Hadley, S. Jabeen, G.Y. Jeng, R.G. Kellogg, J. Kunkle, A.C. Mignerey, S. Nabili, F. Ricci-Tam, M. Seidel, Y.H. Shin, A. Skuja, S.C. Tonwar, K. Wong

Massachusetts Institute of Technology, Cambridge, U.S.A.

D. Abercrombie, B. Allen, V. Azzolini, A. Baty, G. Bauer, R. Bi, S. Brandt, W. Busza, I.A. Cali, M. D'Alfonso, Z. Demiragli, G. Gomez Ceballos, M. Goncharov, P. Harris, D. Hsu, M. Hu, Y. Iiyama, G.M. Innocenti, M. Klute, D. Kovalskyi, Y.-J. Lee, P.D. Luckey, B. Maier, A.C. Marini, C. Mcginn, C. Mironov, S. Narayanan, X. Niu, C. Paus, C. Roland, G. Roland, Z. Shi, G.S.F. Stephans, K. Sumorok, K. Tatar, D. Velicanu, J. Wang, T.W. Wang, B. Wyslouch

University of Minnesota, Minneapolis, U.S.A.

A.C. Benvenuti[†], R.M. Chatterjee, A. Evans, P. Hansen, J. Hiltbrand, Sh. Jain, S. Kalafut, M. Krohn, Y. Kubota, Z. Lesko, J. Mans, N. Ruckstuhl, R. Rusack, M.A. Wadud

University of Mississippi, Oxford, U.S.A.

J.G. Acosta, S. Oliveros

University of Nebraska-Lincoln, Lincoln, U.S.A.

E. Avdeeva, K. Bloom, D.R. Claes, C. Fangmeier, F. Golf, R. Gonzalez Suarez, R. Kamalieddin, I. Kravchenko, J. Monroy, J.E. Siado, G.R. Snow, B. Stieger

State University of New York at Buffalo, Buffalo, U.S.A.

A. Godshalk, C. Harrington, I. Iashvili, A. Kharchilava, C. Mclean, D. Nguyen, A. Parker, S. Rappoccio, B. Roozbahani

Northeastern University, Boston, U.S.A.

G. Alverson, E. Barberis, C. Freer, Y. Haddad, A. Hortiangtham, D.M. Morse, T. Orimoto, T. Wamorkar, B. Wang, A. Wisecarver, D. Wood

Northwestern University, Evanston, U.S.A.

S. Bhattacharya, J. Bueghly, O. Charaf, T. Gunter, K.A. Hahn, N. Odell, M.H. Schmitt, K. Sung, M. Trovato, M. Velasco

University of Notre Dame, Notre Dame, U.S.A.

R. Bucci, N. Dev, M. Hildreth, K. Hurtado Anampa, C. Jessop, D.J. Karmgard, K. Lannon, W. Li, N. Loukas, N. Marinelli, F. Meng, C. Mueller, Y. Musienko³⁶, M. Planer, A. Reinsvold, R. Ruchti, P. Siddireddy, G. Smith, S. Taroni, M. Wayne, A. Wightman, M. Wolf, A. Woodard

The Ohio State University, Columbus, U.S.A.

J. Alimena, L. Antonelli, B. Bylsma, L.S. Durkin, S. Flowers, B. Francis, C. Hill, W. Ji, T.Y. Ling, W. Luo, B.L. Winer

Princeton University, Princeton, U.S.A.

S. Cooperstein, P. Elmer, J. Hardenbrook, N. Haubrich, S. Higginbotham, A. Kalogeropoulos, S. Kwan, D. Lange, M.T. Lucchini, J. Luo, D. Marlow, K. Mei, I. Ojalvo, J. Olsen, C. Palmer, P. Piroué, J. Salfeld-Nebgen, D. Stickland, C. Tully

University of Puerto Rico, Mayaguez, U.S.A.

S. Malik, S. Norberg

Purdue University, West Lafayette, U.S.A.

A. Barker, V.E. Barnes, S. Das, L. Gutay, M. Jones, A.W. Jung, A. Khatiwada, B. Mahakud, D.H. Miller, N. Neumeister, C.C. Peng, S. Piperov, H. Qiu, J.F. Schulte, J. Sun, F. Wang, R. Xiao, W. Xie

Purdue University Northwest, Hammond, U.S.A.

T. Cheng, J. Dolen, N. Parashar

Rice University, Houston, U.S.A.

Z. Chen, K.M. Ecklund, S. Freed, F.J.M. Geurts, M. Kilpatrick, Arun Kumar, W. Li, B.P. Padley, R. Redjimi, J. Roberts, J. Rorie, W. Shi, Z. Tu, A. Zhang

University of Rochester, Rochester, U.S.A.

A. Bodek, P. de Barbaro, R. Demina, Y.t. Duh, J.L. Dulemba, C. Fallon, T. Ferbel, M. Galanti, A. Garcia-Bellido, J. Han, O. Hindrichs, A. Khukhunaishvili, E. Ranken, P. Tan, R. Taus

Rutgers, The State University of New Jersey, Piscataway, U.S.A.

J.P. Chou, Y. Gershtein, E. Halkiadakis, A. Hart, M. Heindl, E. Hughes, S. Kaplan, R. Kunnawalkam Elayavalli, S. Kyriacou, I. Lafotte, A. Lath, R. Montalvo, K. Nash, M. Osherson, H. Saka, S. Salur, S. Schnetzer, D. Sheffield, S. Somalwar, R. Stone, S. Thomas, P. Thomassen

University of Tennessee, Knoxville, U.S.A.

A.G. Delannoy, J. Heideman, G. Riley, S. Spanier

Texas A&M University, College Station, U.S.A.

O. Bouhali⁷³, A. Celik, M. Dalchenko, M. De Mattia, A. Delgado, S. Dildick, R. Eusebi, J. Gilmore, T. Huang, T. Kamon⁷⁴, S. Luo, D. Marley, R. Mueller, D. Overton, L. Perniè, D. Rathjens, A. Safonov

Texas Tech University, Lubbock, U.S.A.

N. Akchurin, J. Damgov, F. De Guio, P.R. Duderov, S. Kunori, K. Lamichhane, S.W. Lee, T. Mengke, S. Muthumuni, T. Peltola, S. Undleeb, I. Volobouev, Z. Wang

Vanderbilt University, Nashville, U.S.A.

S. Greene, A. Gurrola, R. Janjam, W. Johns, C. Maguire, A. Melo, H. Ni, K. Padeken, F. Romeo, J.D. Ruiz Alvarez, P. Sheldon, S. Tuo, J. Velkovska, M. Verweij, Q. Xu

University of Virginia, Charlottesville, U.S.A.

M.W. Arenton, P. Barria, B. Cox, R. Hirosky, M. Joyce, A. Ledovskoy, H. Li, C. Neu, T. Sinthuprasith, Y. Wang, E. Wolfe, F. Xia

Wayne State University, Detroit, U.S.A.

R. Harr, P.E. Karchin, N. Poudyal, J. Sturdy, P. Thapa, S. Zaleski

University of Wisconsin — Madison, Madison, WI, U.S.A.

J. Buchanan, C. Caillol, D. Carlsmith, S. Dasu, I. De Bruyn, L. Dodd, B. Gomber, M. Grothe, M. Herndon, A. Hervé, U. Hussain, P. Klabbbers, A. Lanaro, K. Long, R. Loveless, T. Ruggles, A. Savin, V. Sharma, N. Smith, W.H. Smith, N. Woods

†: Deceased

- 1: Also at Vienna University of Technology, Vienna, Austria
- 2: Also at IRFU, CEA, Université Paris-Saclay, Gif-sur-Yvette, France
- 3: Also at Universidade Estadual de Campinas, Campinas, Brazil
- 4: Also at Federal University of Rio Grande do Sul, Porto Alegre, Brazil
- 5: Also at Université Libre de Bruxelles, Bruxelles, Belgium
- 6: Also at University of Chinese Academy of Sciences, Beijing, China
- 7: Also at Institute for Theoretical and Experimental Physics, Moscow, Russia
- 8: Also at Joint Institute for Nuclear Research, Dubna, Russia
- 9: Now at British University in Egypt, Cairo, Egypt
- 10: Now at Cairo University, Cairo, Egypt
- 11: Now at Ain Shams University, Cairo, Egypt
- 12: Also at Department of Physics, King Abdulaziz University, Jeddah, Saudi Arabia
- 13: Also at Université de Haute Alsace, Mulhouse, France
- 14: Also at Skobeltsyn Institute of Nuclear Physics, Lomonosov Moscow State University, Moscow, Russia
- 15: Also at Ilia State University, Tbilisi, Georgia
- 16: Also at CERN, European Organization for Nuclear Research, Geneva, Switzerland
- 17: Also at RWTH Aachen University, III. Physikalisches Institut A, Aachen, Germany
- 18: Also at University of Hamburg, Hamburg, Germany
- 19: Also at Brandenburg University of Technology, Cottbus, Germany
- 20: Also at Institute of Physics, University of Debrecen, Debrecen, Hungary
- 21: Also at Institute of Nuclear Research ATOMKI, Debrecen, Hungary
- 22: Also at MTA-ELTE Lendület CMS Particle and Nuclear Physics Group, Eötvös Loránd University, Budapest, Hungary
- 23: Also at Indian Institute of Technology Bhubaneswar, Bhubaneswar, India
- 24: Also at Institute of Physics, Bhubaneswar, India
- 25: Also at Shoolini University, Solan, India
- 26: Also at University of Visva-Bharati, Santiniketan, India
- 27: Also at Isfahan University of Technology, Isfahan, Iran
- 28: Also at Plasma Physics Research Center, Science and Research Branch, Islamic Azad University, Tehran, Iran
- 29: Also at Università degli Studi di Siena, Siena, Italy
- 30: Also at Scuola Normale e Sezione dell'INFN, Pisa, Italy
- 31: Also at Kyunghee University, Seoul, Korea
- 32: Also at International Islamic University of Malaysia, Kuala Lumpur, Malaysia

- 33: Also at Malaysian Nuclear Agency, MOSTI, Kajang, Malaysia
- 34: Also at Consejo Nacional de Ciencia y Tecnología, Mexico City, Mexico
- 35: Also at Warsaw University of Technology, Institute of Electronic Systems, Warsaw, Poland
- 36: Also at Institute for Nuclear Research, Moscow, Russia
- 37: Now at National Research Nuclear University ‘Moscow Engineering Physics Institute’ (MEPhI), Moscow, Russia
- 38: Also at St. Petersburg State Polytechnical University, St. Petersburg, Russia
- 39: Also at University of Florida, Gainesville, U.S.A.
- 40: Also at P.N. Lebedev Physical Institute, Moscow, Russia
- 41: Also at California Institute of Technology, Pasadena, U.S.A.
- 42: Also at Budker Institute of Nuclear Physics, Novosibirsk, Russia
- 43: Also at Faculty of Physics, University of Belgrade, Belgrade, Serbia
- 44: Also at INFN Sezione di Pavia^a, Università di Pavia^b, Pavia, Italy
- 45: Also at University of Belgrade, Faculty of Physics and Vinca Institute of Nuclear Sciences, Belgrade, Serbia
- 46: Also at National and Kapodistrian University of Athens, Athens, Greece
- 47: Also at Riga Technical University, Riga, Latvia
- 48: Also at Universität Zürich, Zurich, Switzerland
- 49: Also at Stefan Meyer Institute for Subatomic Physics (SMI), Vienna, Austria
- 50: Also at Adiyaman University, Adiyaman, Turkey
- 51: Also at Istanbul Aydin University, Istanbul, Turkey
- 52: Also at Mersin University, Mersin, Turkey
- 53: Also at Piri Reis University, Istanbul, Turkey
- 54: Also at Gaziosmanpasa University, Tokat, Turkey
- 55: Also at Ozyegin University, Istanbul, Turkey
- 56: Also at Izmir Institute of Technology, Izmir, Turkey
- 57: Also at Marmara University, Istanbul, Turkey
- 58: Also at Kafkas University, Kars, Turkey
- 59: Also at Istanbul University, Faculty of Science, Istanbul, Turkey
- 60: Also at Istanbul Bilgi University, Istanbul, Turkey
- 61: Also at Hacettepe University, Ankara, Turkey
- 62: Also at Rutherford Appleton Laboratory, Didcot, United Kingdom
- 63: Also at School of Physics and Astronomy, University of Southampton, Southampton, United Kingdom
- 64: Also at Monash University, Faculty of Science, Clayton, Australia
- 65: Also at Bethel University, St. Paul, U.S.A.
- 66: Also at Karamanoğlu Mehmetbey University, Karaman, Turkey
- 67: Also at Utah Valley University, Orem, U.S.A.
- 68: Also at Purdue University, West Lafayette, U.S.A.
- 69: Also at Beykent University, Istanbul, Turkey
- 70: Also at Bingol University, Bingol, Turkey
- 71: Also at Sinop University, Sinop, Turkey
- 72: Also at Mimar Sinan University, Istanbul, Istanbul, Turkey
- 73: Also at Texas A&M University at Qatar, Doha, Qatar
- 74: Also at Kyungpook National University, Daegu, Korea